USE OF THE DIFFERENTIAL REFLECTOMETER IN THE STUDY OF THIN FILM CORROSION PRODUCTS ON COPPER

By

CHARLES WILLIAM SHANLEY

A DISSERTATION PRESENTED TO THE GRADUATE COUNCIL OF
THE UNIVERSITY OF FLORIDA
IN PARTIAL FULFILLMENT OF THE REQUIREMENTS OF THE
DEGREE OF DOCTOR OF PHILOSOPHY

UNIVERSITY OF FLORIDA

1977

ACKNOWLEDGEMENTS

The author wishes to express his sincere appreciation to his advisor, Dr. Rolf E. Hummel, for his guidance and confidence throughout this work. Special thanks are extended to Dr. J. B. Andrews for his help in the design and construction of much of the apparatus used in this work, and to Dr. R. J. Nastasi-Andrews for numerous stimulating discussions.

Special thanks are also extended to Dr. E. D. Verink, Jr., for his advice concerning the electrochemical aspects of this research, and to Drs. J. J. Hren, R. Pepinsky, D. B. Dove, and E. D. Verink, Jr., for serving on the author's supervisory committee.

The author wishes to express his appreciation to Dr. B. Cavin, who performed the X-ray analyses mentioned in this work, and to Mr. Patrick Russell, who performed the ellipsometric measurement.

The National Science Foundation provided financial support for this research, which is gratefully acknowledged.

TABLE OF CONTENTS

		Page
ACKNOWLEDGEMENTS		ii
LIST OF TABLES		v
LIST OF FIGURES		vi
ABSTRACT		x
SECTION		
I	INTRODUCTION	1
II	LITERATURE REVIEW	11
	Introduction	11
	Related Techniques	12
	Cuprous Oxide	28
	Band Structure Calculations	28
	Optical Spectroscopy	31
	Growth and Kinetics	37
	Summary	41
III	EXPERIMENTAL PROCEDURE	46
	Introduction	46
	Sample Preparation	47
	Metallographic Preparation	47
	Special Procedures for *In Situ* Samples	50
	Electrolyte Solutions	54
	The Differential Reflectometer	54
	Introduction	54
	The Instrument	56
	Advantages and Disadvantages	59
	Other Equipment	62
	Operating Conditions	66
	Other Considerations	67
	Summary	70

TABLE OF CONTENTS - continued.

	Page
SECTION	
IV RESULTS AND DISCUSSION	72
Introduction	72
Theory of Differential Reflectograms of Thin Films	74
Non-*In Situ* Experiments	95
In Situ Experiments	107
Further Discussion	116
V CONCLUSIONS AND SUGGESTIONS FOR FURTHER WORK	124
REFERENCES	127
BIOGRAPHICAL SKETCH	131

LIST OF TABLES

Table		Page
1	Comparison of Peak Positions for Absorption and Reflection Spectra	32
2	Major Peak Positions in Cu_2O Optical Spectra Compared to Transitions Calculated from the Band Diagram.....	45
3	Composition of Electrolyte Used in Nil Chloride Experiments.....	55
4	Optical Constants $\hat{n} = n+ik$ for Copper and Cupric Oxide (CuO) as a Function of Wavelength.....	83
5	Major Structure in Cu_2O Spectra Obtained from Other Techniques Compared to Differential Reflectometry.....	120

LIST OF FIGURES

Figure		Page
1	Typical experimental arrangement for ellipsometric measurements. The angle ϕ is the angle of incidence.....	13
2	Schematic diagram of a modulated ellipsometer developed by Jasperson et al.[14] The detector (DET) sends the modulated signal to two lock-in amplifiers tuned to 100 KHz and 50 KHz and to a low pass filter. The data is reduced by the computer, C, and displayed on a digital meter, DV. Q' or A' is an additional polarizer used to calibrate the instrument...	17
3	Electrochemical modulation apparatus used by McIntyre.[22]. The HIS 6070 is a computer used to reduce the data.....	22
4	Schematic diagram of a rapid scanning spectrophotometer used by McIntyre et al. See text for details.....	25
5	Band structure diagram for cuprous oxide (Cu_2O) calculated by Dahl and Switendick.....	30
6	Reflectivity spectrum of polished and polished and etched Cu_2O crystals.....	33
7	Electroreflectance spectrum of single crystals of Cu_2O for various AC voltages superimposed on a 1 KV DC bias.....	36
8	Electroreflectance spectrum of Cu_2O at 85 K and no DC bias. The modulating electric field was 60 KV/cm.....	38
9	Schematic diagram of the differential reflectometer.....	57
10	Schematic diagram of the standard corrosion cell used for non-*in situ* experiments.....	63

LIST OF FIGURES - continued.

Figure		Page
11	Schematic diagram of the corrosion cell used for *in situ* experiments. Details of the sample holder are not shown for clarity.....	65
12	Theoretical (Figure 12A) and experimental (Figure 12B) Pourbaix diagrams for copper in nil chloride solutions.....	73
13	Differential reflectogram of a sample prepared in the Cu_2O region of the Pourbaix diagram (-225 mv SCE, pH 9.2, 66 hours).....	75
14	Differential reflectogram of a sample prepared in the CuO region of the Pourbaix diagram (+200 mv SCE, pH 9.2, 18 hours).....	76
15	Typical compositional modulation differential reflectogram. One sample is pure copper, the other copper with 1 at.% aluminum in solid solution.....	77
16	Schematic representation of a typical sample with an oxide film covering half the exposed surface.....	79
17	Variation in $\Delta R/\overline{R}$ as a function of film thickness for a CuO film on a copper substrate. The wavelength of light used is assumed to be 600 nm.....	82
18	Theoretically constructed differential reflectogram of a CuO film 100 Å thick on a copper substrate. λ = 600 nm.....	85
19	Theoretically constructed differential reflectogram of a CuO film 35 Å thick on a copper substrate. λ = 600 nm.....	87

LIST OF FIGURES - continued.

Figure		Page
20	Theoretically constructed differential reflectogram of a CuO film 500 Å thick on a copper substrate. λ = 600 nm.....	88
21	Theoretically constructed differential reflectogram of a CuO film 7500 Å thick on a copper substrate. λ = 600 nm.....	89
22	Variation in $\Delta R/\overline{R}$ as a function of film thickness for a CuO film on a copper substrate over the range d = 0 to 200 Å. The wavelength of light is assumed to be 600 nm.....	91
23	Comparison of the differential reflectogram of an experimentally prepared CuO film (potentiostated at +500 mv SCE at pH 9.2 for 18 hours) to a theoretically constructed reflectogram of a CuO film 25 Å thick.....	93
24	Differential reflectogram of a sample prepared by immersion in distilled water for eighteen hours, with a continuous stream of oxygen bubbled through the water. The structure is characteristic of a mixed oxide of Cu_2O and CuO.....	100
25	Differential reflectograms of three areas of the same sample, which had been potentiostated near the Cu_2O/CuO equilibrium line (-50 mv SCE at pH 9.2) for eighteen hours.....	102
26	Differential reflectogram of a sample potentiostated in the CuO region (A) of the Pourbaix diagram, and of the same sample after the potential has been changed to the Cu_2O region (B). Curve C is the same sample potentiostated for a longer period of time in the Cu_2O region. The baselines of the curves have been shifted for clarity.....	105

LIST OF FIGURES - continued.

Figure		Page
27	Differential reflectograms of two samples potentiostated under the same conditions (5.5 hours at -200 mv SCE, pH 9.2). The first was run in the non-*in situ* cell and measured in air, while the second was prepared and run *in situ*.....	108
28	Differential reflectograms of a sample half covered with a Cu_2O film, showing the sample as measured in air (A), in the empty *in situ* cell (B), and in the *in situ* cell filled with electrolyte (C).....	111
29	*In situ* differential reflectograms of a copper sample potentiostated at -200 mv SCE, pH 9.2, which is in the Cu_2O region of the Pourbaix diagram.....	113
30	Continuation of the *in situ* experiment of Figure 29. Note the change in scale. Since the curves do not change appreciably during these times, the zero lines have been shifted for clarity.....	114

Abstract of Dissertation Presented to
the Graduate Council of the University of Florida
in Partial Fulfillment of the Requirements for the
Degree of Doctor of Philosophy

USE OF THE DIFFERENTIAL REFLECTOMETER IN THE STUDY OF THIN FILM CORROSION PRODUCTS ON COPPER

By

Charles William Shanley

December 1977

Chairman: R. E. Hummel
Major Department: Materials Science and Engineering

An investigation was undertaken to examine the feasibility of using the technique of differential reflectometry to identify and study thin film corrosion products on metal substrates. Differential reflectometry is a form of modulation spectroscopy which measures the normalized difference in reflectivity between two samples, or two adjacent areas of the same sample. In these experiments, one half of each sample was protected by an insulating lacquer while the other half was allowed to form a thin film corrosion product. When the lacquer was subsequently removed, the normalized difference in reflectivity as a function of wavelength was measured over the range λ = 800 nm to 200 nm (1.55 eV to 6.20 eV). The

use of a transparent lacquer permits monitoring of the film *in situ*. Because of the differential nature of the technique, the effect of the metal substrate is subtracted out, so that the resulting differential reflectogram is related to the absorption spectrum of the corrosion product. The similarity in the structure between reflection, absorption, and differential reflectivity spectra substantiates this viewpoint.

In these experiments, copper was chosen as the metal on which the thin film corrosion products were grown. Characteristic spectra for the copper oxides Cu_2O and CuO were obtained, and were used to help define the boundaries of the regions of stability of the copper-water Pourbaix diagram. In addition, the evolution with time of a Cu_2O film was monitored *in situ*.

It was established that in the thickness range of passive and semipassive films (d = 0 to 200 Å) differential reflectometry produces a unique spectrum for each corrosion product, and that the intensity of the structure in the differential reflectogram is related to the thickness of the film. A method is described for calculating the differential reflectograms of thin film corrosion products for various film thicknesses if the optical constants of the film and substrate are known.

Sample spectra are calculated for various thicknesses of a CuO film on a copper substrate. These spectra compare favorably with experimental curves.

SECTION I
INTRODUCTION

Although metallic corrosion is a familiar phenomenon, many aspects of the process remain poorly understood. The reason is not that there is some fundamental bit of information which is lacking; rather, it is that corrosion itself is not a single process. Generally speaking, there are eight basic forms of corrosion,[1] any one or more of which may be present at the same time. The effects may be additive, as when pitting and uniform corrosion attack a holding tank, or even synergistic, as when erosion corrosion and selective leaching attack a brass pipe. In addition, matters taken to eliminate one form of corrosion may inadvertantly introduce new problems, as when the painting of the inside of a tank with a protective coating to eliminate uniform corrosion induces pitting in spots where the coating is imperfect. Altogether, the cost of corrosion in the United States alone is estimated to be in excess of eighty billion dollars annually.[2]

In order to correct a corrosion problem, an engineer must know what kind of corrosion process is present. Frequently, the answer to this question is based on the

identification of the corrosion product. For bulk specimens with massive corrosion, x-ray diffraction techniques, perhaps supplemented by wet chemical analysis, are ordinarily sufficient. Many such bulk corrosion problems are long familiar to the corrosion engineer and may be identified by inspection. For thin films the identification of the corrosion products is considerably more difficult.

It is not uncommon for thin, semipassive layers of corrosion products to form on metals such as aluminum, copper, or silver. Such layers, whether they be oxides, hydroxides, chlorides, or something more complex, are in general insulating or at best semiconducting. Since the aforementioned metals are extensively used by the electronics industry, these thin corrosion films, which form insulating or rectifying contacts on electrical equipment, are of great concern. As in the case of bulk corrosion, the identification of the corrosion product is the first step in solving the corrosion problem.

Unfortunately, such films are frequently difficult to analyze. X-ray diffraction techniques, which probe as much as a millimeter into the surface of a specimen, will often not show up an oxide layer on the outer one hundred thousandth millimeter of the surface. A more surface sensitive, less penetrating form of spectroscopy is called for.

Electron spectroscopy techniques seem to provide the answer. Auger Electron Spectroscopy (AES) and Electron Spectroscopy for Chemical Analysis (ESCA) are the most commonly used techniques. Both have certain advantages over x-ray techniques for the study of thin films. Auger analysis and ESCA penetrate only a few atomic distances (typically around 25 Å) into the sample. This makes them well-suited for thin film analysis. Auger spectroscopy is not particularly well-suited for the identification of specific compounds, but ESCA, as its name implies, can identify compounds as well as elements. If the AES or ESCA apparatus is equipped with an ion milling device, the evolution with depth of the thin film corrosion product may be also studied. Both techniques are precise, well-known, and the apparatus is readily available.

No technique is without its limitations, and AES and ESCA are not exceptions to this rule. The equipment for either is expensive and complex, and requires trained operators. They are both destructive techniques, in that an electron or ion beam abrades away the sample. They are not particularly fast. However, their most fundamental problem is that they require the sample to be placed in a vacuum.

Removing a sample from its normal environment for study is a common research technique, but it is never done

without a certain amount of misgivings. The boundary conditions are changed, and the results may not be the same as if the study were performed *in situ*. If a titanium or aluminum specimen with an oxide coating is placed into a vacuum chamber, there will probably be no change in the oxide layer. However, if a sample with a fragile hydroxide layer or a complex compound containing water of hydration is removed from an electrolyte and exposed to air for a few hours, it is likely that the compound will not remain the same. If the sample is placed in a vacuum chamber and evacuated to 10^{-7} torr, the probability of changes in the sample approaches certainty. Some analytical technique which does not require a vacuum, and can hopefully be used for *in situ* analysis, is clearly needed.

Optical techniques may provide a solution in such cases. Many of these thin film corrosion products are semitransparent to the eye. This implies that the films preferentially absorb certain wavelengths of light in the visible region of the spectrum. This absorption could be the basis for the analysis of the thin films. In addition, optical techniques have other advantages over x-ray or electron spectroscopy.

A light beam penetrates typically fifty atomic distances (around 100 Å) into a metal. It penetrates a much

further distance through a semitransparent film, making it suitable for examining the entire depth of the film without penetrating extensively into the metal substrate. In addition, optical techniques are non-destructive techniques. But the greatest advantage of optical techniques is that they do not require a vacuum; indeed, the proper technique can study a sample *in situ*.

Traditionally, ellipsometry has been the optical technique used to study thin films on substrates. This technique measures the degree to which a film changes plane polarized light into elliptically polarized light, and the phase difference between the two components of the elliptically polarized light. Using this information, ellipsometry can calculate any two of the three parameters n, k and d, where n is the index of refraction, k is the index of absorption, and d is the thickness of the film. Computerized iteration techniques permit the determination of all three parameters, but the process is not rapid. High speed computer-controlled ellipsometers, although expensive, have improved this situation somewhat.[3]

One technique, differential reflectometry,[4] provides fundamentally different information when compared to ellipsometry, or for that matter, to AES or ESCA. By

monitoring the difference in reflectivity between two samples as a function of wavelength, a series of peaks is obtained, each of which represents a transition from one energy band to another in the sample. If one sample is clean metal and the other sample metal with a thin film of corrosion product on it, measurement of the difference in reflectivity should show only the effect of the corrosion product. Since each compound is presumed to have a unique set of energy levels, this technique can identify the presence of a corrosion product, its identity, and its evolution with time. The measurements may be performed *in situ*, if need be. In addition, it is nondestructive, fast, and does not require a vacuum.

In addition to studies on existing corrosion problems, the technique of differential reflectometry is useful to corrosion engineers in other ways. Pourbaix diagrams are often used to represent a large amount of thermodynamic data concerning corrosion in an easy-to-interpret form. Such a diagram is a plot of potential versus pH, and shows regions of thermodynamic stability for metals and their associated corrosion products. A Pourbaix diagram may be constructed from thermodynamic data on the metal and corrosion products with the aid of the Nernst equation,

$$E = E_0 + \frac{RT}{nF} \ln \frac{[a_{ox}]}{[a_{red}]}$$

where E is the half-cell potential, E_0 is the standard half-cell potential, R is the gas constant, T is the absolute temperature, n is the number of electrons transferred, F is the Faraday constant, and $[a_{ox}]$ and $[a_{red}]$ are the activities (concentrations) of the oxidized and reduced species.

This equation is used to define regions of thermodynamic stability in the Pourbaix diagram. It is well-known, however, that many real physical processes do not take place under equilibrium conditions. Hence the equilibrium diagram may not apply. Therefore it is of great interest to the corrosion engineer as well as the thermodynamicist to construct experimental Pourbaix diagrams to which the thermodynamically correct Pourbaix diagram may be compared. This experimental diagram is a practical guide which may be useful in engineering applications as well as being a comparative measure of how closely experimental conditions approach equilibrium conditions.

Experimental Pourbaix diagrams are normally constructed using the potentiodynamic method.[5] At a fixed value of pH, the potential of the sample relative to some convenient reference is slowly varied while the current

through the sample (which is directly proportional to the corrosion rate) is monitored. A plot of applied potential versus the logarithm of the corrosion current is normally obtained on an x-y recorder. If the potentiodynamic scan is begun with the potential applied to the sample well into the immunity region of the Pourbaix diagram, the corrosion current should be essentially zero. As the potential becomes more cathodic and the sample moves out of the immunity region, the corrosion current should increase. Any abrupt change in the corrosion current signals the formation or dissolution of a corrosion product. For example, a sudden decrease in the corrosion current of several orders of magnitude as the potential is made more cathodic may indicate the onset of passivity at that potential and pH. Numerous scans at different values of pH serve to establish the experimental Pourbaix diagram.

One difficulty with this technique is that although the formation of a corrosion layer may be observed, the identity of that corrosion product is not determined. If the corrosion product forms in or near a region of the Pourbaix diagram where a certain product is expected it is not unreasonable to assign that product to that area of the experimental Pourbaix diagram. However, borderline cases or conflicting results are not uncommon, as is a

good deal of experimental scatter. Independent verification of the corrosion product is essential. Specimens prepared potentiostatically are inherently closer to equilibrium than potentiodynamically varied samples, and may be analyzed to determine the identity of the corrosion product. Since many of these films are too thin for x-ray analysis, optical methods represent the only simple techniques for examining these films without resorting to a vacuum. Because differential reflectometry seems to produce a unique set of peaks for each corrosion product, it should be possible to identify corrosion products present in various regions of the experimental Pourbaix diagrams. In addition, *in situ* techniques make possible the study of kinetics of film dissolution or formation.

Initial studies of any new technique must be made on carefully selected samples. Copper was chosen as the metal upon which the films would be formed, since copper has fairly well-characterized corrosion products, most of which have a visible color which implies absorption bands in the visible region. In addition, theoretical and experimental Pourbaix diagrams have been established.

It is the purpose of this work to investigate the feasibility of using the technique of differential reflectometry to identify and characterize thin film corrosion

products on metal substrates. In addition, the concept of using potentiostatic electrochemical techniques in conjunction with differential reflectometry to delineate areas of stability in experimental Pourbaix diagrams is to be investigated. To this end, the advantages of differential reflectometry, such as speed, freedom from vacuum requirements, and, most importantly, the possibility of true *in situ* measurements, are used to supplement conventional potentiostatic and potentiodynamic research techniques. Differential reflectometry provides a technique for the direct observation of corrosion phenomena, thereby supplementing the indirect technique of potentiodynamic scans. In this respect it is similar to x-ray diffraction, which can provide a direct way of studying phase changes in materials which are indirectly indicated by resistometric or differential thermal analysis (DTA) techniques.

No single technique, or combination of techniques, can be applied to the study of all corrosion phenomena. It is believed, however, that differential reflectometry, by supplementing the information obtained using more conventional techniques, will provide a rapid, reliable, and more complete means of studying thin film corrosion phenomena.

SECTION II
LITERATURE REVIEW

Introduction

In the development of a new analytical technique, two problems must be considered—the mechanics of the technique itself and the interpretation of the results of that technique. Therefore, this review will be divided into two major parts. The first is a discussion of several optical methods which have been developed for the study of thin films. Their chief advantages and disadvantages, as well as how they relate to differential reflectometry, will be discussed. Most of these techniques are useful primarily for the study of very thin films and seek to find the optical constants n and k and the thickness, d, of the film. Differential reflectometry seeks only the identity of the film and its thickness, without regard for the particular optical constants.

The second part of this review will concentrate on optical studies of cuprous oxide, Cu_2O. In order to identify thin film corrosion products with the differential reflectometer, one must know the absorption spectra or optical constants of each corrosion product as

a function of wavelength. This initial study has concentrated on the oxides of copper, Cu_2O and CuO. Of the two, Cu_2O has been more extensively studied since it possesses an intrinsically interesting electronic structure. Cuprous oxide, Cu_2O, has a rich exitonic spectrum as well as a fundamental energy gap in the visible area of the spectrum. (An exiton is a bound electron-hole pair produced by some semiconductors by the absorption of an appropriate wavelength of light.) Cupric oxide, CuO, has not been as extensively studied. Fortunately, one study which has been done provides the optical constants as a function of wavelength, something which has not been done for Cu_2O.[6]

Related Techniques

The traditional method for investigating thin films on substrates has been ellipsometry. In a typical experimental arrangement, shown in Figure 1, a monochromatic light beam passes through a polarizer to produce plane polarized light. This light is reflected from the metal or metal/film surface at the angle of incidence, ϕ, producing elliptically polarized light. This elliptically polarized light may be visualized as two perpendicular plane polarized waves of amplitude ratio ψ and phase difference Δ. These ellipsometric parameters are determined

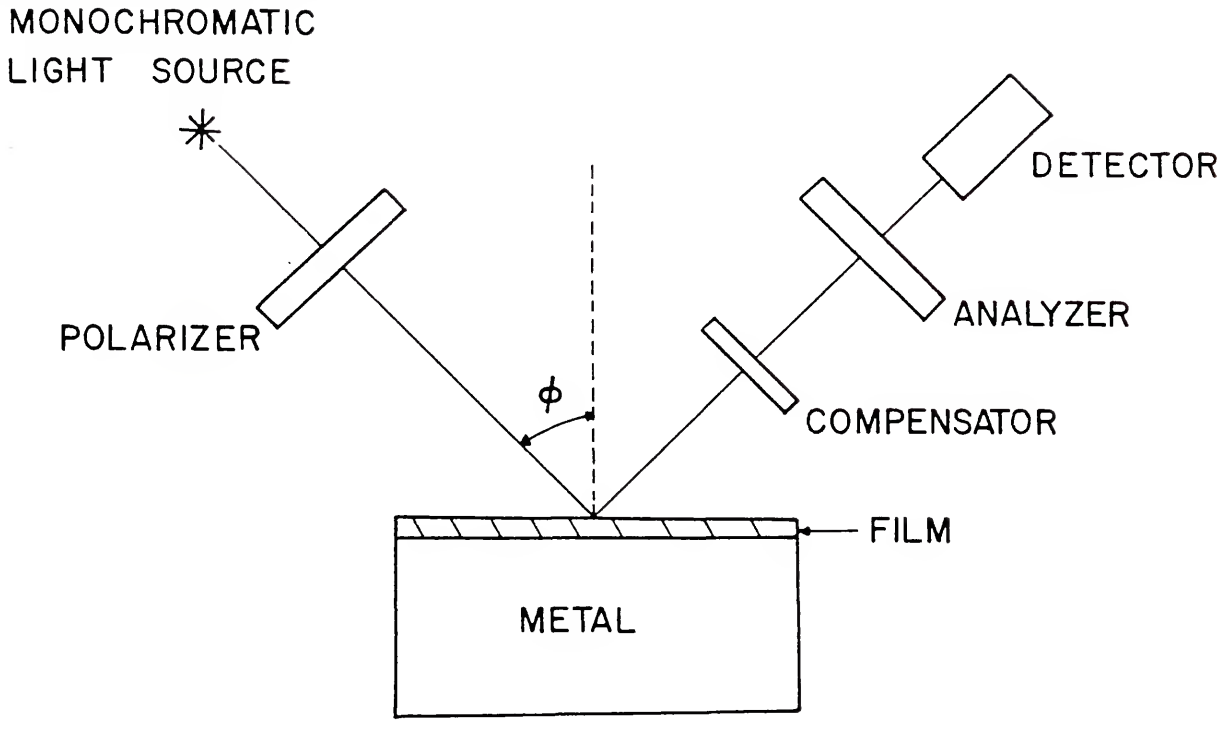

Figure 1. Typical experimental arrangement for ellipsometric measurements. The angle ϕ is the angle of incidence.

by the optical constants of the metal and film, as well as the thickness of the film. The phase difference, Δ, between the two plane polarized waves can be brought to zero by appropriate adjustments of the compensator, producing a single plane polarized wave again. The analyzer is then rotated so as to extinguish the plane polarized light, and the resultant values of Δ and ψ determined from the compensator and analyzer settings. The values of Δ and ψ are then used to calculate the optical constants n and k.

The situation is not quite as simple as this, of course. The values of Δ and ψ by themselves are insufficient to uniquely determine n, k, and d for the film. Until recently, the film thickness, d, had to be determined independently, by coulometry, interferometry, or a series of ellipsometric measurements. None of these methods are particularly easy, and all are time-consuming.[7] However, Paik and Bockris[8] have shown that the ratio of the intensity of the light reflected from the film parallel to the plane of incidence ($r_{||}$) to that polarized perpendicular to the plane of incidence ($r_{\perp}$) can be used in addition to ψ and Δ to determine the unknowns n, k and d. Unfortunately, only a few existing automatic ellipsometers, such as those of Paik and Bockris[8] and Cahan and Spanier,[3] can easily measure these quantities.

A new approach by O'Handley[9] and O'Handley and Burge[10] calculates the effective reflectivity from Δ and ψ and uses this quantity in addition to Δ and ψ to find the three unknowns, n, k, and d, for the film. As O'Handley points out, two possible values of the film thickness, d, can be produced using this analysis, but since they often differ by an order of magnitude, only a general idea of the thickness of the film is necessary to unambiguously determine all three parameters.

Another feature of the classic ellipsometer which has made it less than ideal for thin film investigations is its lack of speed. In electrochemical investigations, many reactions occur very fast, and the determination of Δ and ψ for a classic ellipsometer may require many minutes. Modifications to the normal operation of an ellipsometer, such as off-null techniques,[11] can increase the sensitivity to transients and facilitate the monitoring of known films, but more exotic techniques are required for unknown films of very rapid film formation.

One approach to the problem is to speed up classical ellipsometry. Such an approach has led to a series of automatic ellipsometers, such as that of Cahan and Spanier,[3] and recently to a commercial instrument.[12] These instruments, which often use a continuously rotating

analyzer and a dedicated minicomputer, can analyze a film for n, k, and d in four to ten seconds.[12] Their chief drawback is their expense, since a commercial automatic ellipsometer costs approximately $20,000, or about four times the cost of a conventional ellipsometer.[13]

Various kinds of modulation techniques have also been employed to speed up ellipsometry. The modulated parameter is ordinarily the polarization of the light beam, which is varied by a photoelastic crystal[14] or by a Faraday cell.[15] Alternately, an oscillating analyzer[16] or polarizer may be used. Figure 2 shows one such modulated ellipsometer developed by Jasperson et al.[14] It is similar to a standard ellipsometer except that instead of a normal compensator it uses a piezoelectrically-driven quartz crystal to modulate the phase shift of the light beam. The detector uses two lock-in amplifiers to simultaneously monitor the reflectivity at the modulation frequency (50 KHz) and at twice the modulation frequency (100 KHz). In addition, the DC reflectivity is also monitored using a low pass filter in order to take into account changes in source intensity, detector response, and so on. The 50 KHz and 100 KHz signals contain information from which n and k for the film may be derived if the thickness, d, is known. If it is not, the method

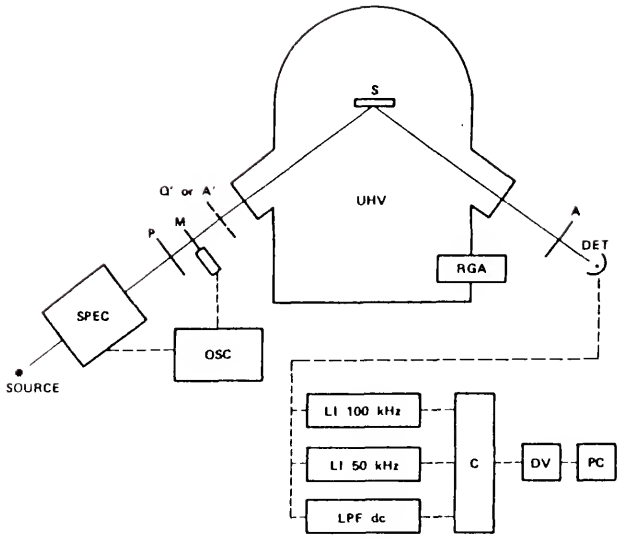

Figure 2. Schematic diagram of a modulated ellipsometer developed by Jasperson et al.[14] The detector (DET) sends the modulated signal to two lock-in amplifiers tuned to 100 KHz and 50 KHz and to a low pass filter. The data is reduced by the computer, C, and displayed on a digital meter, DV. Q' or A' is an additional polarizer used to calibrate the instrument.

of O'Handley[9] may be used to find n, k, and d simultaneously.[10] The instrument is said to be an order of magnitude more precise than standard ellipsometers and can measure Δ and ψ in less than thirty seconds.[14]

Differential reflectometry, as used in the study of thin film corrosion products, is similar to the related technique of differential reflection spectroscopy used by McIntyre and others.[17-19] Differential reflection spectroscopy, however, uses polarized light and seeks to find the optical constants $\hat{n} = n + i\,k$ for the film, while differential reflectometry does not require polarized light and seeks only the reflection spectrum of the film to identify it.

As in differential reflectometry, the differential reflection spectroscopy technique of Kolb and McIntyre[19] measures the normalized difference in reflectivity,

$$\frac{\Delta R}{R} = \frac{R_1 - R_2}{R_1}$$

where R_1 is the reflectivity of the metal and R_2 the reflectivity of the metal/film composite. The difference in reflectivity is normalized by dividing by the reflectivity of the metal rather than the average reflectivity. Additional information may be obtained by polarizing the light beam parallel to $[(\frac{\Delta R}{R})_{||}]$ and per-

pendicular to $[(\frac{\Delta R}{R})_{\perp}]$, the plane of incidence. McIntyre and Aspnes[18] have shown that if the film thickness is very small relative to the wavelength of light being used, then

$$(\frac{\Delta R}{R})_{\perp} = \frac{8\pi\ d\ n_0\ \cos\phi}{\lambda}\ \mathrm{Im}(\frac{\hat{\varepsilon}_1-\hat{\varepsilon}_2}{\varepsilon_0-\hat{\varepsilon}_2}) \qquad (1)$$

and

$$(\frac{\Delta R}{R})_{||} = \frac{8\pi\ d\ n_0\ \cos\phi}{\lambda}\ \mathrm{Im}\{\frac{\hat{\varepsilon}_1-\hat{\varepsilon}_2}{\varepsilon_0-\hat{\varepsilon}_2}[\frac{1-\frac{\varepsilon_0}{\hat{\varepsilon}_1\hat{\varepsilon}_2}(\hat{\varepsilon}_1+\hat{\varepsilon}_2)\sin^2\phi}{1-(\frac{1}{\hat{\varepsilon}_2})(\varepsilon_0+\hat{\varepsilon}_2)\sin^2\phi}]\} \qquad (2)$$

where ϕ is the angle of incidence. The surrounding phase (either air or electrolyte) has a real dielectric constant, ε_0, and index of refraction, n_0, while the thin absorbing film and substrate metal have complex dielectric constants, $\hat{\varepsilon}_1$ and $\hat{\varepsilon}_2$, respectively.

Using these equations, there are two methods for measuring the optical constants of the film.

1. Measure the two quantities $(\frac{\Delta R}{R})_{\perp}$ and $(\frac{\Delta R}{R})_{||}$ at a single angle of incidence.

2. Measure either $(\frac{\Delta R}{R})_{\perp}$ or $(\frac{\Delta R}{R})_{||}$ at two or more angles of incidence.

The details of each kind of measurement have been given by Kolb and McIntyre.[19] Method 2 is not used because of mathematical difficulties in extracting the

optical constants n and k. Method 1 has been used successfully to study adsorbed layers on gold 6 Å thick.[19]

This technique has certain advantages over conventional ellipsometry which are similar to the advantages of differential reflectometry, such as easily performed measurements *in situ*, fast response time, and measurements over a range of wavelengths. However, it is a difference technique rather than a differential technique because the reflectivity of the metal and the metal/film composite is not measured at the same time. The reflectivity of the clean metal surface is measured in air, rather than *in situ*. The sample cell is filled with electrolyte and the sample potentiostated in the desired region of the Pourbaix diagram. After an appropriate amount of time, the reflectivity is again measured as a function of wavelength for both polarizations of light. The normalized difference in reflectivity is then calculated point by point by computer.

Several points need to be considered when comparing differential reflectance spectroscopy to differential reflectometry. In differential reflectance spectroscopy, two scans over the entire wavelength range are necessary to determine the complex dielectric coefficient of the film, in addition to the reflectivity measurements and

Kramers-Kronig calculation necessary to obtain the optical constants of the substrate.[18] Secondly, the output is not a continuous curve, but only a series of points. Sharp changes can be missed. Thirdly, if the film is absorbing, the thickness must be determined independently before n and k for the film can be obtained. Finally, equations 1 and 2 are only accurate if $d/\lambda \leq .003$.[18] For λ = 250 nm (approximately the lowest wavelength used in this work) d must be less than 7.5 Å. Hence the technique is useful mainly for studying adsorbed monolayers. Semi-passive films such as CuO or Cu_2O are often over 100 Å thick,[20] and even passive layers such as those found on stainless steel are often around 30 Å in thickness.[21] In addition, since in most cases the absorption coefficient, k, is greater than zero, the thickness, d, of the film must be independently determined before the optical constants n and k can be found. However, this technique does measure the optical constants of the film, which is something differential reflectometry does not do.

Another popular technique is that of electrochemical modulation spectroscopy (EMS).[22] Here, the modulated parameter is the electrode potential, cell current, or the surface charge of the sample. In its most common form (Figure 3) it is used to measure adsorption on metal

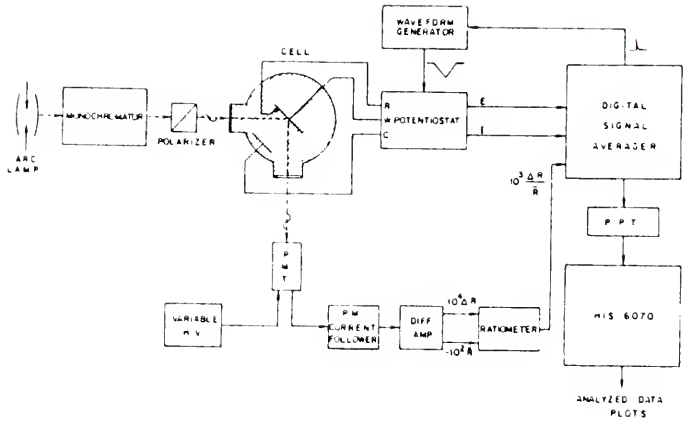

Figure 3. Electrochemical modulation apparatus used by McIntyre.[22] The HIS 6070 is a computer used to reduce the data.

substrates, such as hydrogen on rhodium or iridium,[23,24] or oxygen on gold, platinum, or nickel electrodes.[19,25,26] Light from a Xenon arc lamp passes through a monochromator and polarizer and into the optical cell, where it is reflected from the metal surface and collected outside the cell by a photomultiplier tube. The potential of the sample is controlled by a potentiostat which can be modulated by an external waveform generator. At a signal from an on-line minicomputer, the waveform generator imposes a triangular pulse on the voltage supplied to the sample. The reflectivity as well as the cell current and the electrode potential are digitized and recorded by the minicomputer at 256 time intervals. A number of sweeps (typically 64) are made to increase the signal to noise ratio, and the data is reduced by computer to a plot of $\frac{\Delta R}{R}$ versus λ. As in the case of differential reflectance spectroscopy, the output is in the form of a series of points rather than a smooth curve.

Although electrochemical modulation appears to be an excellent method of studying adsorbed layers, two limitations should be noted. First, the reaction must be truly reversible. The formation of an oxide which does not readily dissolve, for example, must be avoided. Second, the reaction must be fast enough to be affected by the

modulation. (Typical modulation conditions are a sawtooth wave, 44 mv peak to peak at 43 Hz.[27]) For fast, reversible reactions, however, this technique works well.

Internal reflection spectroscopy has been used to study adsorption on thin film substrates such as gold[28] or platinum.[29] In internal reflection spectroscopy, a light beam is internally reflected in a transparent substrate. At the point of reflection, the light beam interacts with the film on the other side of the substrate, and the resultant changes in the light beam may be used to characterize the film. For example, Hansen[28] has observed the adsorption of molecular dyes on thin (100 Å) layers of gold. In addition, electrochemical modulation techniques may be used with internal reflection spectroscopy to study fast, reversible reactions. Such a technique was used by McIntyre and Peck[29] to observe the adsorption of hydrogen on platinum films 100 Å thick in .5 M H_2 SO_4. The beauty of the technique is that the observations are made from the electrode side of the interface.

Rapid scanning spectroreflectometry is a new development which permits the continuous measurement of reflection spectra over a wide wavelength range. A recent instrument used by McIntyre[24] is shown in Figure 4. A rapidly scanning galvanometer mirror (GM) sweeps a high

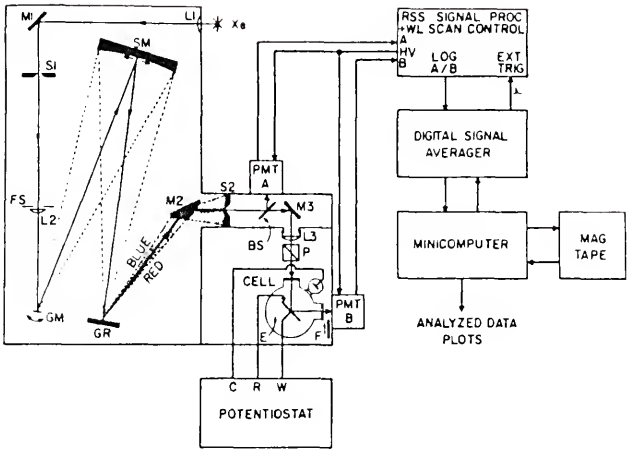

Figure 4. Schematic diagram of a rapid scanning spectrophotometer used by McIntyre.[24] See text for details.

intensity beam of white light across the surface of a spherical mirror (SM). The reflected beam is focused by the spherical mirror onto a diffraction grating (GR) at a fixed position, but at a variable angle of incidence. This produces a wide beam of quasi-monochromatic light which is scanned across the exit slit at speeds up to 1000 Å/ms. A beam splitter (BS) permits the simultaneous measurement of the incident light intensity via photomultiplier A (PMT A) and the reflected intensity via photomultiplier B (PMT B). The signals are sampled in the time domain (which is related to the wavelength by the oscillation frequency of the mirror) by a minicomputer. The normalized difference in reflectivity, $\frac{\Delta R}{R}$, of the film free surface (obtained earlier and stored in the computer) and the film covered surface is calculated and displayed. Normally a signal averaging technique is used, wherein typically 512 wavelength scans are used to enhance the signal to noise ratio. Rapid reflectivity changes can be observed, since even with signal averaging a typical scan takes less than one minute. One important advantage of the technique is that surface roughening, such as is possible with electrochemical modulation spectroscopy, is avoided since the electrode potential is not modulated. However, since the scan is so rapid, the

high voltage supplied to the photomultiplier tubes cannot be easily adjusted to maintain the average output voltage at an optimum level. As a result, precision may suffer when the light intensity is low.

One final effect common to all these techniques is the possibility of electroreflectance effects complicating the reflectance spectra of the film/metal surface of samples measured *in situ*. For such samples, the electroreflectance effect can arise from two sources:[22] changes in the dielectric constant of the metal at the surface due to the capacitance of the electrical double layer between the bulk metal and the bulk electrolyte; and, a change in the refractive index of the solution at the ionic double layer. High DC as well as AC potentials can produce these effects.[27] The electroreflectance effect can be a valuable probe of the metal surface, or an unfortunate complication of the thin film absorption spectra, depending on what is being investigated. The effect does not subtract out of the reflection spectrum when the difference techniques described in this section are employed because the reflectivities of the samples are measured under different conditions. Evidence will be presented in Section III which indicates that the technique of differential reflectometry may not produce electroreflectance

peaks because the reflectivities of the samples are measured at the same time and under similar conditions.

Cuprous Oxide

Band Structure Calculations

Theoretical studies of the band structure of Cu_2O have been made by Zhilich and Makarov,[30] Elliot,[31] and Dahl and Switendick.[32] The early work of Zhilich and Makarov[30] treated only the $\Gamma'_{25} \rightarrow \Gamma_1$ transition, where Γ'_{25} is assumed to be the top of the valence band, and Γ_1 the bottom of the conduction band. This is generally agreed to be the fundamental energy gap of Cu_2O, and gives the oxide its red color. This band gap, calculated according to the method of Kohn and Rostoker[33] was found to be 2.38 eV, in good agreement with the experimentally determined 2.2 eV.[30]

Elliot[31] did not calculate transition energies, but instead presented a simple, qualitative band structure derived from symmetry conditions of the cuprous oxide lattice. Both direct and indirect transitions were considered.

By far the most ambitious attempt at the calculation of the energy levels of Cu_2O has been by Dahl and Switendick.[32] They calculated the energies of a very

large number of energy levels, using the augmented plane wave (APW) method proposed by Slater,[34] with muffin tin potentials. Their band calculations show the $\Gamma_{25}' \rightarrow \Gamma_1$ transition to have an energy of 1.77 eV, somewhat below the experimental 2.2 eV. Figure 5 shows the calculated band structure. Not all the possible transitions are allowed, and of those which are permitted, many are insufficiently intense to be observed. For information on which transitions do occur, one must investigate the optical spectra of Cu_2O and attempt to correlate observed structure with possible transitions. The major difficulty here is that while band structure calculations are often qualitatively correct, the assigned energies for favorable transitions are frequently rather imprecise. As mentioned previously, in the calculations of Dahl and Switendick,[32] the $\Gamma_{25}' \rightarrow \Gamma_1$ transition, which is generally agreed to be the transition defining the fundamental gap in Cu_2O, is found to have an energy of 1.77 eV. Experimentally, the gap is found to be 2.2 eV – a difference of half an electron volt. Hence while band structure calculations can provide a useful qualitative picture of the structure of a thin film differential reflectogram, quantitative data is best obtained from optical spectroscopy.

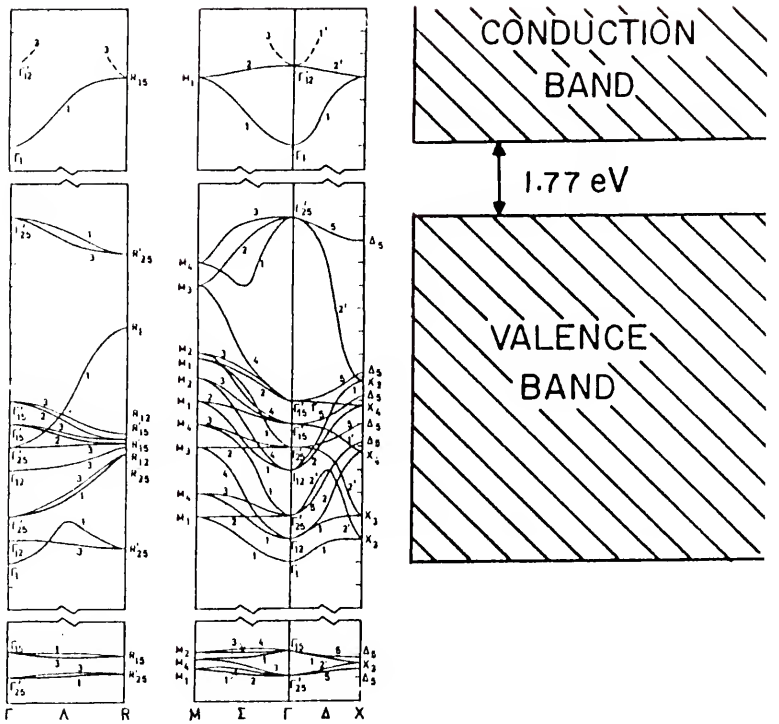

Figure 5. Band structure diagram for cuprous oxide (Cu_2O) calculated by Dahl and Switendick.[32]

Optical Spectroscopy

Brahms and Nikitine[35] have measured the absorption and reflectance spectra for single crystals of Cu_2O in the 2.5-6.5 eV region. Absorption was measured at 77 K and 295 K, and reflection at 77 K. A good deal of peak sharpening occurs in the absorption spectra at low temperatures. The correlation between peak positions for absorption spectra and reflection spectra as shown in Table 1 is quite good, as it must be. The authors associate the transitions at 2.58, 2.62, 2.71, 2.74, and 4.33 eV with exiton formation. The strong peak at 5.52 eV is attributed to a maximum in the joint density of states.

Balkanski, Petroff, and Trivich[36] have measured the reflectivity of Cu_2O in the ultraviolet (2-25 eV) at 300 K, and the reflectivity in the visible (200-500 nm) at 30 K. They then use the Kramers-Kronig relationship to determine ε_2 for the 2.5-6 eV region of the spectrum at 30 K. The reflectivity data for Cu_2O at 30 K corresponds well to the earlier work of Brahms and Nikitine.[35] Both mechanically polished as well as polished and etched samples were measured, as shown in Figure 6. It is evident that most of the structure, including all of the exiton peaks, is dependent upon the surface state of the

Table 1

Comparison of Peak Positions for Absorption and Reflection Spectra[35]

Absorption Peaks [eV]	Reflectivity Peaks [eV]
2.61	2.58
	2.62
2.71	2.71
	2.75
3.62	3.62
	3.9
4.33	4.33
4.48	4.48
4.74	4.74
4.86	4.86
4.94	4.94
	5.08
5.36	5.39
5.52	5.53
5.79	5.84
6.45	

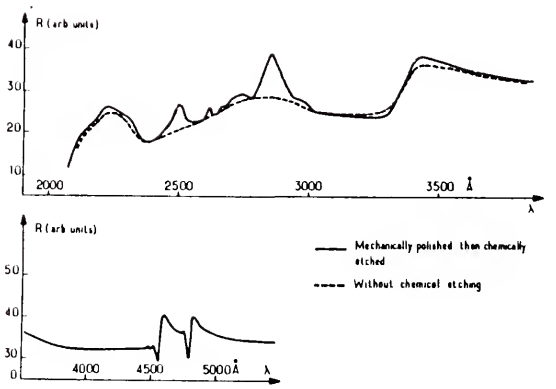

Figure 6. Reflectivity spectrum of polished and polished and etched Cu_2O crystals.[36]

sample. No exitonic structure appears for unetched specimens. This point is very significant since it implies that exitonic structure might not be observed in the current experiments, or that at least the structure may not be sharp and well-defined. Thus only two areas of structure would remain from which to identify the oxide Cu_2O: the broad transitions at 340 nm (3.64 eV) and at 225 nm (5.51 eV). The 3.64 eV structure may be due to a transition at a high symmetry point, such as $X_{3T} \rightarrow X_{3C}$. The theoretical value calculated by Dahl and Switendick[32] for this transition is 3.5 eV. The broad peak around 5.56 eV is thought to be due to another transition from a high symmetry point, such as R.

Zouaghi, Prevot, Carabatos, and Seiskind[37-39] measured the infrared absorption[37] and photoconductivity[38] of Cu_2O after annealing in oxygen for different times and temperatures. They observed changes in the absorption and photoconductivity with different oxygen concentrations and annealing times, which implies that the method of formation of Cu_2O may influence its optical spectra. Hence the reflection and absorption spectra of Brahms and Nikitine[35] and of Balkanski et al.,[36] which were thermally grown, may not be identical with the spectra of electrochemically prepared specimens.

In addition to reflectivity and absorption measurements, some electroreflectance data has been obtained for Cu_2O. Shestatskii and Sobolev[40] have examined the electroreflectance of polycrystalline Cu_2O from 3.3 to 4.5 eV (375-275 nm). Even in this short range, two strong peaks were observed, at 3.6 eV (344 nm) and 4.25 eV (292 nm). These agree fairly well with the reflectivity data in that interval of Brahms and Nikitine[35] and Balkanski et al.[36] Shestatskii, Sobolev, and Likhobabin[41] measured the electroreflectance of Cu_2O single crystals at 77 K. The thin, etched samples were studied at various modulation voltages and DC bias voltages. Peaks were observed in the 2.5-2.8 eV(496-443 nm) range which were identified as exiton peaks. Unfortunately, no measurements were performed on unetched samples. Both the shape of the peaks and their polarity were found to be dependent on modulating voltage and DC bias. A representative set of spectra is shown in Figure 7, for various AC voltages and a constant 1 KV DC voltage.

A somewhat larger spectral region, from about 2.5 to 6.0 eV (500-200 nm), was measured by Daunois, Deiss, and Nikitine.[42] They measured the electroreflectance of bulk, polished, and etched samples at 85 K. A large number of peaks were observed, most of which agree well with re-

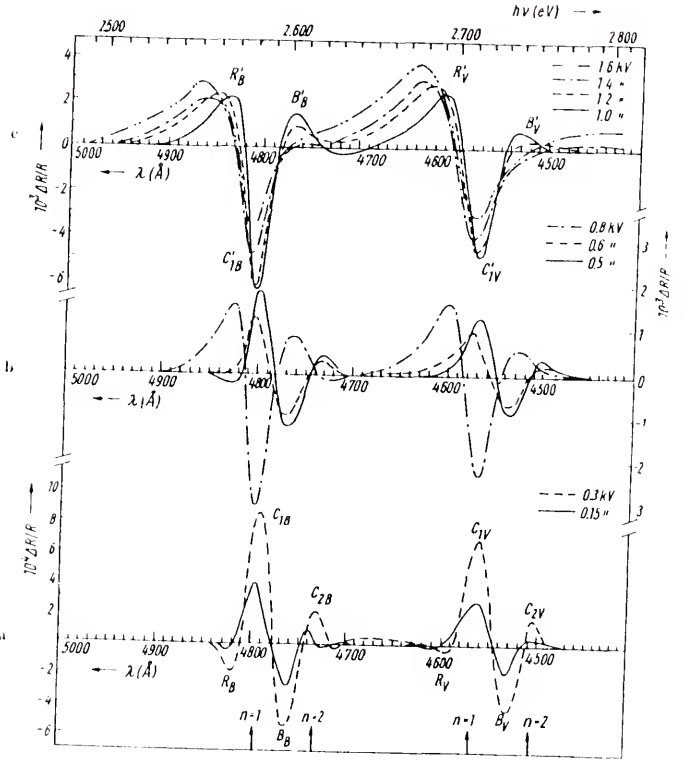

Figure 7. Electroreflectance spectrum of single crystals of Cu_2O for various AC voltages superimposed on a 1 KV DC bias.[41]

flectivity data. Figure 8 shows the electroreflectance spectrum at 85 K. The structure is well-defined and very rich.

Growth and Kinetics

The preparation of standard films of various copper oxides is an important step in calibrating the differential reflectometer for corrosion studies of copper. When the band structure of the oxide is known, it should be possible to identify the oxide by the optical properties as recorded by the differential reflectometer. In other cases a standard film of known composition is needed to determine the standard spectra. One method of obtaining a standard film is to potentiostat the base metal under specific corrosion conditions which, according to the Pourbaix diagram, might be expected to produce the correct corrosion film. In the case of oxides, heating the base metal in oxygen may be sufficient.

Ebisuzaki[43] prepared large single crystals of Cu_2O from large slices of single crystal copper. The technique involved high temperatures (980°C) and low partial pressures of oxygen (3.1 mm Hg in a nitrogen atmosphere). Other thermally grown oxides were made by Wieder and Czanderna.[44] Most oxides were mixtures of Cu_2O, CuO, and $CuO_{.67}$ (which is apparently a defect structure Cu_2O).

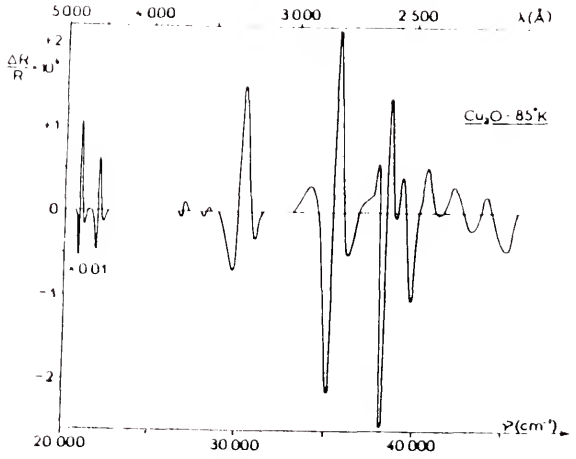

Figure 8. Electroreflectance spectrum of Cu_2O at 85 K and no DC bias. The modulating electric field was 60 KV/cm.[42]

X-ray investigations showed that in the early stages of oxidation the crystals produced were amorphous. This implies that thermally grown oxides may not have a well-defined crystal structure and hence not a well-defined band structure during early stages of growth.

In most of these cases of thermally grown Cu_2O, the aim was to produce bulk samples, rather than thin films. Electrochemical methods are probably better suited to growing thin films on copper substrates than thermal methods, since electrochemical methods tend to produce films which are more dense and compact. Characterization of the film is, as usual, the major problem.

The growth of oxide films of spherical single crystals of copper in distilled water was studied by Kruger.[20, 45,46] Using a special oscillating crystal technique he was able to establish that Cu_2O was the film formed on copper in distilled water exposed to air. This is the same oxide which is slowly formed when copper is exposed to air. Further, when pure oxygen was bubbled through the water, the film initially produced was Cu_2O. This is not unreasonable since any CuO which begins to form would tend to be reduced to Cu_2O by the copper substrate. These Cu_2O films were observed to form very rapidly and reach a limiting thickness after about two

hours. The precise film thickness, as measured by standard ellipsometric techniques, varied with the crystallographic orientation of the copper, but averaged about 90 Å for this case. After long times a porous, loosely adherent CuO layer was observed to form on the Cu_2O layer. The formation of the CuO overlayer apparently did not prevent the continued growth of the Cu_2O underlayer. One variable was found to influence the growth of Cu_2O, however: light.

Cuprous oxide is a p-type semiconductor. Since its band gap of 2.2 eV is in the visible part of the electromagnetic spectrum (about 560 nm, or yellow-green) it is not unexpected that light might have some effect on its electronic properties. That these electronic properties affect the kinetics of growth is somewhat more surprising. When Cu_2O films are illuminated by the appropriate wavelength of light, electrons are transferred from the valence band to the conduction band, where they can migrate to the copper electrode. This process inhibits the growth of the Cu_2O film by a process not completely understood. Whatever the exact mechanism may be, inhibition of Cu_2O growth has been observed by Kruger on single crystals of copper.[45,46] Similar results were obtained by Ives and Rawson[47] for polycrystalline copper. Kruger's work with

single crystals showed a decrease in Cu_2O film thickness of about one-third for samples illuminated by a 500 watt tungsten light over similar samples which were not illuminated. No effect on the film growth rate was observed if the distilled water was kept saturated with oxygen. Attempts to employ a monochromator with the light source to determine the spectral response of the inhibition of film growth were not successful due to the lack of light intensity. This implies that monitoring film growth with the differential reflectometer or an ellipsometer probably would not inhibit the growth of a Cu_2O film.

Summary

Of the several methods related to differential reflectometry which may be used to investigate thin film corrosion products, ellipsometry is the most common. In its basic form, ellipsometry can determine the optical constants n and k to a high degree of precision if the thickness of the film is known. Recent advances have eliminated even that requirement, provided the absolute reflectivity can be measured,[8] or if a reasonable guess can be made as to the thickness of the film.[9,10] Very precise values of n, k, and d may thus be determined from

a classical, well-established instrument. The only remaining drawback is the slow speed of the classical ellipsometer, and even this barrier is being overcome through the use of automatic[3] and modulated[14-16] ellipsometers.

For thin adsorbed films, many spectroscopic techniques are available. Differential reflection spectroscopy[17-19] is very similar to differential reflectometry, but employs polarized light and measures the reflectivity before and after film formation rather than concurrently. Although it can determine the optical constants, it can only do so for very thin monolayer films.

For the study of fast, reversible reactions *in situ*, electrochemical modulation[19,23-26] is ideal. Here an adsorbed film is induced to form and redissolve by modulations of the electrode potential. Its only real disadvantage is that the number of possible applications is small. Also somewhat limited in application is internal reflection spectroscopy, which has the unique advantage of observing film formation from the electrode side of the interface. Its chief limitation is that light must pass through the electrode. Finally, for very fast reactions or transient phenomena, rapid scanning spectroreflectivity can be a useful method of measuring changes in reflectivity.

Some such techniques have the advantage over differential reflectometry in that they can determine the optical constants of the thin film corrosion product. Some, such as electrochemical modulation or rapid scanning spectroreflectivity, can study very rapid reactions. However, all except ellipsometry are more or less limited to very thin (monolayer) films. Such films are important in studies of catalysis and adsorption, but passive and semipassive layers are too thick to be analyzed for n and k using these techniques. Differential reflectometry is well-suited to the study of these films in the 5 Å-500 Å range, but requires some way other than the optical constants to identify the film.

Several avenues are open to one wishing to identify thin film corrosion products with differential reflectometry. Some, such as x-ray or various forms of electron spectroscopy, were discussed in Section I. Other methods include the correlation of peak position with either band structure data, or reflectivity spectra.

The most complete band structure study of Cu_2O is that of Dahl and Switendick.[32] While it agrees well qualitatively with observed structure in the reflectivity spectrum, the energies of transitions do not. More detailed calculations are required before band structure

data alone may be used to identify corrosion products without additional data from reflectivity curves.

Several techniques have been used to record the optical spectra of Cu_2O. Most agree on the major structure, but various techniques differ in their sensitivity to exiton structure and to complications from electroreflectance effects. The data of Balkanski et al.[36] is most important since it shows that structure due to exiton formation may not be visible in unetched specimens.

Table 2 summarizes the reflectivity data and band structure calculations discussed in this section. Only room temperature data are shown. The calculations of Dahl and Switendick[32] are shown shifted so that the fundamental gap occurs at the experimental energy, with the original data in parentheses. This translation may not be correct, but probably results in more accurate values than the original calculation. It is given here as an approximation only. Agreement between the different experimental techniques is good, which implies that peaks at similar positions should be visible in differential reflectograms of Cu_2O.

Table 2

Major Peak Positions in Cu_2O Optical Spectra Compared to Transitions Calculated from the Band Diagram (see text)

Reflectivity[36]	ε_2[36]	Electroreflectance		Calculated[32]
		Ref. 40	Ref. 42	
2.5	2.7	-	2.59 2.73	2.25 (1.77)
3.4	-	3.35 3.60	3.66 3.77	3.84 (2.86)
3.7	3.7	3.78 3.95	-	3.74 (3.26)
4.3	4.4	4.08 4.25	4.35 4.90	4.41 (3.63)
4.7	4.8	-	4.72 4.76 4.92	4.83 (4.35)
5.0	5.3	-	5.03 5.21	5.07 (4.59)

SECTION III
EXPERIMENTAL PROCEDURE

Introduction

Any analytical technique must be capable of consistent results. Frequently this is the most difficult aspect of the development of a new technique, since unexpected variables in the experimental process may produce inconsistent results. The application of differential reflectometry to corrosion studies is particularly susceptible to this problem for three reasons—it involves thin films, electrochemistry, and a new analytical technique.

One reason thin films of corrosion products are difficult to study is because they are difficult to detect. They are known to be delicate, often easily altered, and frequently nonuniform, either across the specimen or in depth profile. Electrochemical techniques, being thermodynamic in nature, are easily influenced by small changes in experimental conditions. For example, unexpected temperature changes or power interruptions may produce anomalous results. Finally, the analysis technique, differential reflectometry, while well-established

for compositional modulation studies of alloys,[48-51] has never been applied to electrochemical studies.

It is therefore of the utmost importance that the sample preparation and experimental procedure be carried out in a careful and consistent manner, in order that the results be as reproducible as possible.

Sample Preparation

Metallographic Preparation

Copper samples were prepared from a 3/4" (19 mm) diameter bar of 99.999% pure copper.* Each sample was lathe cut from the bar to form a dish 3/4" (19 mm) in diameter and approximately 3/8" (9.5 mm) thick. In order to eliminate any possible contamination by the cutting operation, each dish was immersed in 20% nitric acid for fifteen hours. A small, 1/16" (1.6 mm), hole was drilled in the back of the sample to a depth of about 3/16" (4.8 mm) to facilitate the attachment of the electrode wire.

Each sample was then ground flat with a succession of 180, 320, and, finally, 600 grit silicon carbide papers. Grinding was accomplished on a metallographic

*Obtained from the A. D. McKay Corp., New York, New York.

polishing wheel while the papers were lubricated with liquid soap and water. Due to the fact that the silicon carbide particles tend to become embedded in soft materials such as copper, the minimum amount of polishing necessary to properly finish the specimen was performed. Since it was found that even these measures did not eliminate silicon carbide embedding, further polishing was performed using Microcut paper.* Microcut paper is a mildly abrasive, napped paper which produces a surface finish similar to 600 grit silicon carbide paper, but contains no silicon carbide or other particulate abrasives. The cutting action is a product of the nap of the cloth alone. By polishing each sample for a sufficiently long period of time on several pieces of Microcut paper lubricated with liquid soap and water, it was found that virtually all silicon carbide contamination could be eliminated, as confirmed by microscopic examination. Fortunately such elaborate measures were found to be necessary only during the first polishing of the as-cut specimens. Used specimens with mild amounts of corrosion in the form of thin film layers could be cleaned with Microcut paper alone. As mentioned above, this produced

*Microcut paper, trademark of Buehler, Ltd., Evanston, Illinois

a sample with a finish similar to that produced with 600 grit silicon carbide paper, but without the silicon carbide contaminants. Such a finish completely removed all traces of the thin films studied in this work.

After polishing with Microcut paper, each sample was fine-polished with 6 micron followed by 1 micron diamond paste on a felt cloth using Metadi* fluid as a lubricant. This polishing technique produced a uniform, mirror-like finish on the sample.

In order to fasten the sample wire to the specimen, a tiny brass fitting was constructed. The fitting was in the form of a truncated cone with a maximum diameter of about 1/16" (1.6 mm). The sample wire, which was insulated with Teflon** to ensure freedom from attack by the electrolyte, was soldered to the end of the fitting. This assembly could be attached to the sample by means of a press fit. Finally, the fitting and most of the sample were covered with a special lacquer (Miccroflex***) which previous experience had indicated would not be affected by

*Metadi fluid, trademark of Buehler, Ltd., Evanston, Illinois
**Teflon, trademark of E. I. DuPont, Wilmington, Delaware
***Miccroflex, trademark of Michigan Chrome and Chemical Co., Detroit, Michigan

the electrolyte and would prevent the covered section of the sample from corroding.

Special Procedures for *In Situ* Samples

Samples prepared for *in situ* analysis require an optically transparent layer for the insulating coating, since the light beam must be able to see a corroded and an uncorroded part of the sample at the same time while the sample is in the electrolyte. It was eventually established that collodion provided the most satisfactory coating.

From a theoretical point of view, quartz would seem to provide the best coating. It is optically transparent, insulating, and very resistant to chemical attack. However, quartz cannot be easily deposited on the copper surface. Extensive attempts to sputter quartz on the sample face were not successful due to the nature of the sputtering process. When quartz, SiO_2, is sputtered off a quartz target, SiO_2 particles are not the only species produced. The momentum transfer process which makes sputtering possible partially dissociates the SiO_2 into Si, O, O_2, and SiO as well as the predominant SiO_2. The resulting free oxygen in the chamber reacts with the copper sample before a protective layer of SiO_2 can be

deposited. The result is oxidized copper, covered with an insulating SiO_2 layer. The effect is enhanced by the high temperature of the plasma and the high energies imparted to the oxygen ions by the sputtering action. In addition, in order to obtain SiO_2 layers free from SiO contamination, the manufacturer* suggests adding additional oxygen to the system and sputtering in an oxygen enriched argon atmosphere. This only provides more oxygen to oxidize the copper before a protective layer is formed. (The situation is no problem to the major user of quartz sputtering equipment, the semiconductor industry, since they are generally sputtering onto silicon.)

Silicon monoxide, SiO, was another unsuccessful candidate. Although it can be evaporated instead of sputtered, it is not entirely optically transparent. A SiO coating has a yellow-brown tint which is readily detected by the differential reflectometer. Attempting to evaporate SiO in an oxygen enriched atmosphere and deposit SiO_2 on the sample produces only the oxidation and destruction of the boat used to evaporate the SiO.

Evidently some kind of mechanically applied chemical compound similar to Miccroflex but transparent was

*Perkin-Elmer Co., Palo Alto, California

necessary. Miccroflex may be thinned out to a great extent and still remain protective, but it also remains purple. The color may not be apparent to the eye, but the differential reflectometer shows it quite clearly. Other commercial compounds used in electroplating such as Miccroshield* showed similar results.

It is known that Tygon tubing, noted for its chemical resistance, can be liquified by the chemical Tetrahydrafluoran (THF). This can then be readily applied to specimens by a dip method, and subsequent air drying restores the physical and chemical properties of the original Tygon. Transmissivity studies showed it to be transparent from 800 to approximately 350 nm, which encompasses much of the present range of the instrument. Unfortunately, the dissolved Tygon would not dry to a uniform thickness. This produced interference colors on the film which completely obscurred any differential reflectometry data. Attempts to produce films of Tygon thinner than about 2000 Å in order to eliminate the interference effect produced films with no appreciable degree of adherence to the copper sample. This led to a small

*Miccroshield, trademark of Michigan Chrome and Chemical Co., Detroit, Michigan

gap between the copper and the "protective" film, causing massive crevice corrosion.

Thus far the most satisfactory coating has been found to be collodion, a waxy organic compound used to make replica specimens for transmission electron microscopy. It is available dissolved in either amyl acetate or alcohol and may be thinned to any desired degree by the addition of additional solvent. Since alcohol of extremely high purity is easily obtained, and has the advantage of rapid drying time, it was chosen over amyl acetate as the solvent for this work. Collodion layers may be deposited on half the sample by the simple method of dipping half the sample in the dissolved collodion. The collodion then dries to a uniformly thick, fairly adherent layer in about thirty seconds.

The physical properties of the collodion layer are similar to the Tygon coatings. Thick layers will produce interference colors due to non-uniformity of the film. Extremely thin layers have little adherence to the copper sample, and produce crevice corrosion. The advantage of collodion over Tygon is that the collodion is more readily dissolved, dries faster, and produces more uniform films. Even so, a film sufficiently thin to minimize absorption of the light beam and eliminate interference

colors will break down or loose adherence after twenty-four to forty-eight hours in the electrolyte. Further research in this area of transparent, insulating coatings is clearly needed.

Electrolyte Solutions

Electrolyte solutions were prepared from reagent grade chemicals and distilled water which had been passed through two ion exchange columns. Typical resistivity was on the order of 10^6 ohms·cm. Nil chloride solutions were prepared according to Table 3.

Immediately before use electrolytes were deoxygenated by vacuum deaeration. All beakers, flasks, and corrosion cells used for nil chloride work were used only for nil chloride work, and were periodically cleaned with nitric acid to ensure freedom from chloride contaminants.

The Differential Reflectometer

Introduction

The differential reflectometer is a device which measures the difference in reflectivity of two samples as a function of wavelength. The technique is a form of modulation spectroscopy where the modulated parameter is the surface composition of the samples. Originally de-

Table 3

Composition of Electrolyte Used
in Nil Chloride Experiments

pH	Buffer	NaOH	
4	100 ml 1.0 M KHP	-	
5	100 ml 1.0 M KHP	108 ml .5 M	
6	100 ml 1.0 M KHP	180 ml .5 M	
7	143 ml 0.7 M H_3BO_3	10 ml .1 M	dilute to 2000 ml
8	143 ml 0.7 M H_3BO_3	100 ml .1 M	
9	143 ml 0.7 M H_3BO_3	100 ml .5 M	
10	143 ml 0.7 M H_3BO_3	184 ml .5 M	
11	132 ml 0.7 M H_3BO_3	220 ml .5 M	

veloped to monitor changes in the band structure of metals with alloying,[48-51] it is used here to investigate the growth of thin films of corrosion products on metal substrates. In this case the differential reflectometer scans a light beam between two areas of the same sample, one of which is clean and the other covered with a thin film of corrosion product. The reflectivity of the copper substrate, which is common to both sides of the sample, does not contribute to the differential reflectogram, while the absorption spectrum of the corrosion product does contribute.

The Instrument

A schematic diagram of the instrument used in this work is shown in Figure 9. Light from a high pressure Xenon light source* is passed through a scanning monochromator** and reflected by a flat mirror onto an oscillating mirror. The oscillating mirror scans the light beam across the two areas of the sample at a frequency of 60 Hz. The size of the area to be scanned can be varied by changing the voltage applied to the mirror.

*Xenon light source, Mc Pherson model 613, 75 W, Mc Pherson, Inc., Acton, Massachusetts
**Grating monochromator, Mc Pherson model 218, Mc Pherson, Inc., Acton, Massachusetts

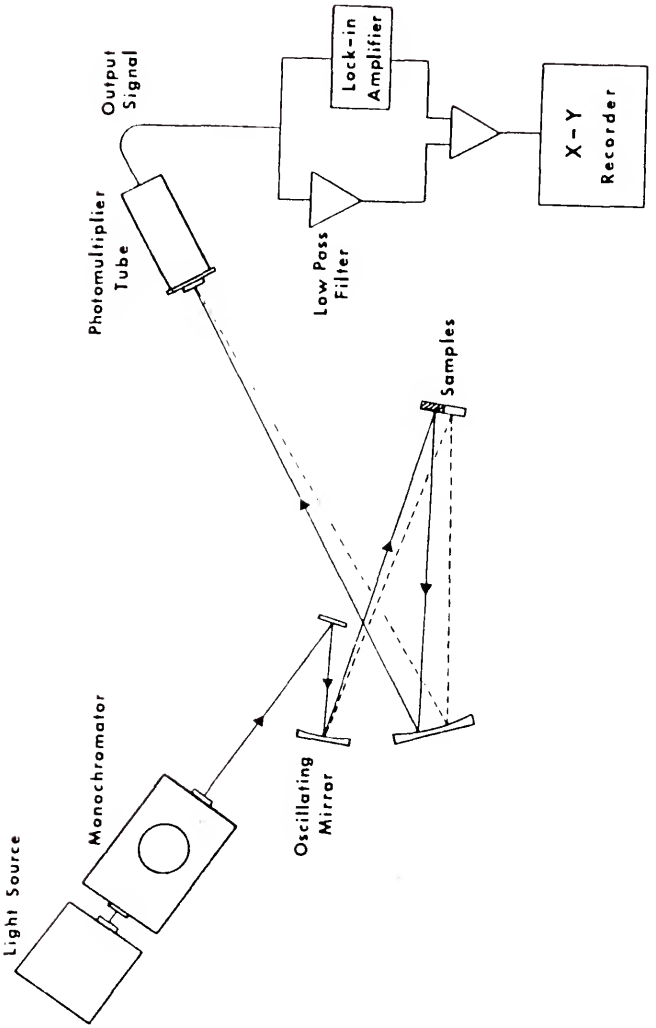

Figure 9. Schematic diagram of the differential reflectometer.

Normally the total area scanned is about 2x4 mm. In the present work, one area of the sample is clean copper, and the other copper with a thin layer of corrosion product on top. The reflected light is focused on a frosted quartz plate in front of the photomultiplier tube.* The purpose of the frosted plate is to diffuse the light across the face of the photocathode, since the response of the photocathode normally varies across its surface. The signal from the photomultiplier is of the form of a square wave superimposed on a DC signal. This output signal is split into two channels. The first passes into a lock-in amplifier which is tuned to the frequency of the oscillating mirror. This produces a slowly varying DC signal whose amplitude is proportional to the square wave component of the signal from the photomultiplier. The output from the photomultiplier is also passed through a low pass filter, which smoothes out the AC signal and produces an output whose amplitude is proportional to the average reflectivity, $\bar{R}$. These two signals are then combined in a divider circuit to produce the $\Delta R/\bar{R}$ signal, which is plotted on the y-axis of an x-y recorder. A voltage from the monochromator supplies the signal to the x-axis of the

*Photomultiplier tube, EMI extended S-20 type, EMI, Inc., Middlesex, England

recorder proportional to the wavelength, λ. In its present form, the differential reflectometer scans a wavelength range of 200 to 800 nm (6.2-1.6 eV) in about one and one-half minutes.

The differential reflectometer used in this work is an improved version of the instrument described elsewhere.[4] The chief improvements are the substitution of mirrors for lenses in order to eliminate chromatic aberation, and a new monochromator to improve resolution. Improvements to the electronics have also been made to maintain the average output voltage of the photomultiplier at a constant level by varying the applied voltage automatically.

Advantages and Disadvantages

Conventional optical studies of corrosion products have typically been performed using ellipsometric techniques. As mentioned in the introduction, this technique can determine the thickness, d, of a thin film if its optical constants n and k are known. Layered films, however, may confuse the issue by giving anomalous values for n and k. In addition, for *in situ* studies, the effect of the absorption spectra of the electrolyte and windows must be taken into account. Finally, conventional ellipsometry is not particularly rapid.

Differential reflectometry, on the other hand, has certain advantages over ellipsometry. Among these are the speed of the analysis and the fact that each corrosion product appears to have a unique differential reflectogram. However, the most important advantage of the technique is that it is a differential technique, so that all factors contributing to the reflectivity which are common to both sides of the sample cancel out. For example, the electrolyte solution which the light beam passes through during *in situ* measurements has an absorption spectrum which is a function of wavelength. If e_1 and e_2 are the voltage levels produced by the photomulitplier tube when it is illuminated by the light reflected from the two halves of the sample, and $\alpha(\lambda)$ is the function describing the absorption of the electrolyte as a function of wavelength, then

$$e_1 = \alpha(\lambda)\ R_1(\lambda)$$

and

$$e_2 = \alpha(\lambda)\ R_2(\lambda)$$

where R_1 and R_2 are the reflectivities of the first and second half of the specimen, respectively.

Thus,

$$\frac{e_1-e_2}{\left(\frac{e_1+e_2}{2}\right)} = \frac{\alpha(\lambda)R_1-\alpha(\lambda)R_2}{\left(\frac{\alpha(\lambda)R_1+\alpha(\lambda)R_2}{2}\right)} = \frac{R_1-R_2}{\left(\frac{R_1+R_2}{2}\right)} = \frac{\Delta R}{\bar{R}} \qquad (3)$$

The effect of the absorption spectrum of the electrolyte cancels out. This argument also holds for other "machine parameters" such as the spectral output of the lamp and the response of the photomultiplier, both of which are also a function of wavelength. In addition, recent improvements to the instrument such as matching the time constant of the ΔR and $\overline{R}$ channels have reduced the effect of transients such as line voltage fluctuations.

The technique of differential reflectometry is not without its limitations, however. Since it requires a "standard" or reference sample, it may be difficult to implement in some cases. When compared to ellipsometry, it does not seem possible to determine the optical constants of the film.

When compared to electron spectroscopy, differential reflectometry lacks the ability to analyze the surface of the thin film, since light penetrates the film to a greater extent than an electron beam. This also implies that no depth profile of the film may be made. In addition, the analyzed area is presently 2 mm square on each half of the specimen, which eliminates the possibility of analyzing microscopically small areas of the sample. Finally, for *in situ* analysis, a transparent lacquer must be used to cover the "clean" or reference half of the

sample. This is difficult to achieve in practice, and even a seemingly transparent film will absorb a light beam to some extent. This is acceptable if no additional structure is added to the differential reflectogram.

In conclusion, each experimental technique offers certain advantages over the others. It is believed that differential reflectometry can compliment the better known techniques of AES, ESCA, and ellipsometry.

Other Equipment

Standard techniques were used for the electrochemical parts of this study. Figure 10 shows a schematic of the conventional corrosion cell used in this work. The body of the cell is made of glass which had been cleaned with Chromerge* and rinsed with concentrated nitric acid to remove surface contaminants. A hard rubber stopper on the top of the cell has ports for pyrex tubes which can accommodate the sample electrode wire and bright platinum auxiliary electrode wire. A Luggin probe, or salt bridge, contains electrolyte and is connected to the small electrode reservoir outside the corrosion cell where the saturated calomel reference electrode is located. Pro-

*Chromerge, trademark Manostat, Inc., New York, New York

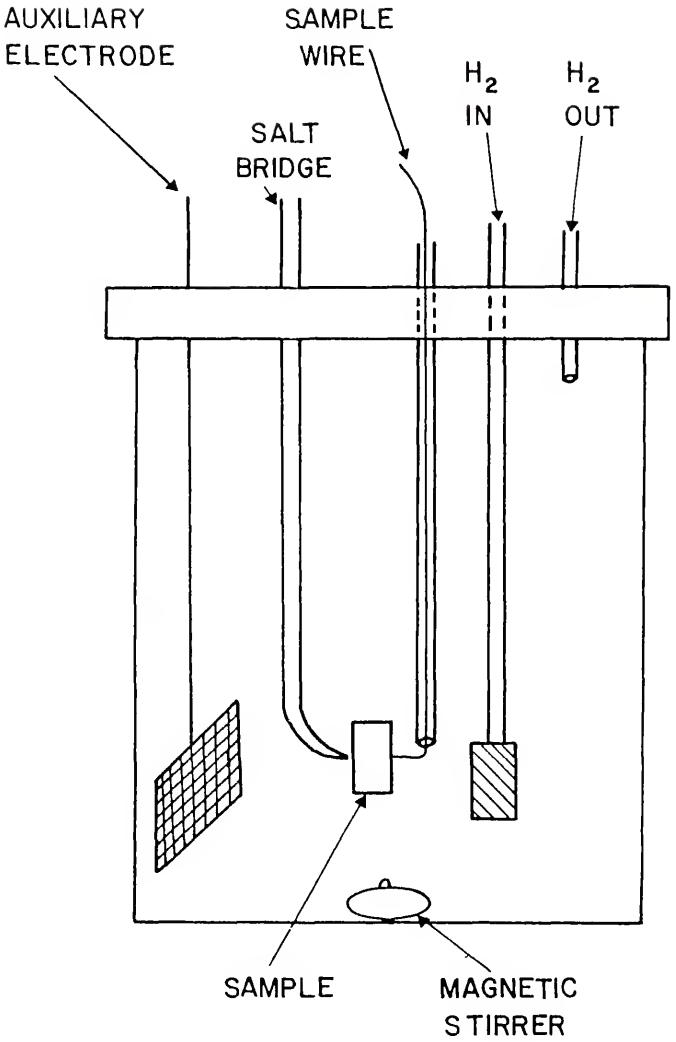

Figure 10. Schematic diagram of the standard corrosion cell used for non-*in situ* experiments.

visions are also made for a thermometer and for a fritted glass gas diffuser, whose purpose is to bubble hydrogen through the electrolyte and keep it deoxygenated. A Teflon encapsulated magnetic stirrer maintains circulation in the electrolyte.

Figure 11 shows the corrosion cell designed for the *in situ* examination of thin film corrosion products. The major differences between the *in situ* cell and the conventional corrosion cell are the addition of a quartz window for the entering and exiting light beam and a Teflon sample holder to keep the sample rigidly fixed at the focal point of the oscillating mirror. In addition, the auxiliary or platinum electrode is in the form of a ring around the sample in order that it does not interfere with the light path. The only materials which are in contact with the electrolyte other than the sample are made of quartz, Pyrex, Teflon, Tygon, or covered with Miccroflex.

The potentiostat used in these experiments was designed and constructed in-house and was based on earlier similar designs. The purpose of any potentiostat is to maintain a constant potential difference between the sample electrode and the reference electrode, which in this case was a saturated calomel electrode. In order to

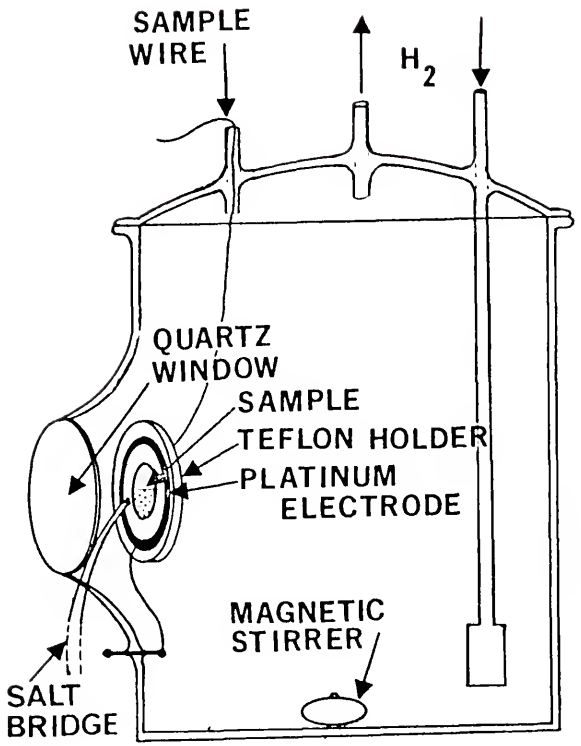

Figure 11. Schematic diagram of the corrosion cell used for *in situ* experiments. Details of the sample holder are not shown for clarity.

maintain the potential difference, sufficient current is applied from the auxiliary (platinum) electrode to keep the voltage drop through the electrolyte between the sample and the reference electrode at the desired value. The potentiostat constructed for this work can maintain a potential within one millivolt of the desired value for periods in excess of three days, and contains special temperature compensating circuits to eliminate voltage drift over all reasonable temperature fluctuations. Finally, it presents an unusually high input impedance to the reference electrode of 10^{12} ohms.

Operating Conditions

Samples were prepared for normal or *in situ* analysis as described previously. Approximately 700 ml of electrolyte was deaerated by vacuum deaeration and transferred to the corrosion cell. In most cases, the sample was placed in the cell and the potential between the sample and reference electrode adjusted so as to put the operating conditions in the immunity region of the Pourbaix diagram (such as, 550 mv SCE at pH 9.2). Under these conditions, the stable species is copper, and no corrosion product should form. After approximately five minutes, the potential was changed to the value desired

for the experiment in as short a period of time as possible. Hydrogen gas was bubbled through the electrolyte at the rate of approximately 5 cc/sec. at all times to keep the solution deoxygenated. In addition, the electrolyte was continuously stirred by the Teflon encapsulated magnetic stirrer. Only during actual *in situ* measurements were these operations suspended, in order to reduce mechanical vibration in the cell.

After potentiostating for the desired amount of time, samples not to be measured *in situ* were removed from the cell, rinsed with distilled water, and dried with filtered, dry air. They were then immediately measured with the differential reflectometer. Time between removal of the sample from the cell and measurement of the differential reflectogram was typically two minutes.

Other Considerations

Any new analysis technique typically has a number of problems which must be resolved before the technique can be reliably applied. In this case, the problems may conveniently be divided into two areas: those related to electrochemistry and those related to the differential reflectometer.

It is well-known that electrochemical techniques have certain problems associated with them due to the nature of

the techniques. For example, the saturated calomel reference electrode must contain a truly saturated solution of potassium chloride (KCl) in the electrode reservoir or it will not provide a stable reference voltage. In order to assure this condition, a small amount of KCl crystals are kept in the electrode tip to maintain complete saturation. A similar problem exists with the salt bridge, or Luggin probe. If the resistivity of the electrolyte solution is high, there will be a voltage drop between the tip of the probe in the corrosion cell and the calomel electrode at the other end of the probe. This effect, which would lead to the incorrect potential being applied to the sample, has been minimized in this work by the careful design of a very high impedance input to the potentiostat. This reduces current drain from the calomel electrode to the picoamp range, so that a relatively high resistivity in the electrolyte may be tolerated without an appreciable voltage drop. However, the potentiostat is susceptible to both power failures, which are generally detectable, and reductions in line voltage, which are not so readily detected. If the voltage to the potentiostat is sufficiently reduced, the potential supplied to the sample can shift in unpredictable ways. If undetected, this may lead to

erroneous results. Continuous voltage monitoring and multiple tests at each point in the Pourbaix diagram help identify this problem.

Another difficulty which is difficult to resolve is the possibility of film formation during the moments between sample immersion and activation of the potentiostat, and the similar problem of film formation while the potentiostat is being adjusted to the desired potential. For example, after coating half the sample with Miccroflex, approximately twenty minutes must pass before the lacquer is completely dry. During this time, a thin layer of air-formed oxide can form on the exposed half of the sample. Attempts to observe this film using the differential reflectometer have not been successful, which indicates that if the film does exist, it must be very thin. Nonetheless, as was previously mentioned, it has been general practice in this work to "pre-potentiostat" the sample in the immunity region of the Pourbaix diagram for a few minutes prior to the actual experiment in order to encourage dissolution of this hypothetical film. Referring to the Pourbaix diagram of Figure 12, however, it is clear that to adjust the potential from the immunity region to the CuO region, the potential must pass through the Cu_2O region. If a Cu_2O film forms rapidly, it

may interfere with the formation of the CuO film. This transition time spent in the undesired region of the Pourbaix diagram may be minimized but not eliminated. The fastest rates obtainable are limited by the inherent time constant of the potentiostat to one to two seconds.

Experimental considerations concerning the differential reflectometer are relatively straightforward. While a differential reflectogram is being made of an *in situ* sample, the hydrogen being bubbled through the electrolyte must be stopped and the magnetic stirrer turned off to eliminate mechanical vibrations which increase the amount of electronic noise in the system. In addition, since it is well-known that light can affect the growth of the thin film corrosion products,[20,46,47] light from the monochromator must be blocked except when actual measurements are being made.

Summary

The differential reflectometer was used to measure the difference in reflectivity between the corroded and uncorroded areas of electrochemical specimens. The specimens were prepared using standard metallographic techniques, with extra care being used to eliminate carbide embedding and sample contamination. Electrolyte solutions

were prepared from reagent grade chemicals and deaerated before use. Normal as well as *in situ* corrosion cells were designed to have only inert substances in contact with the electrolyte. A plot of the normalized difference in reflectivity of the clean half of the sample minus the corroded half can be obtained as a function of wavelength over the spectral range 800-200 nm.

SECTION IV
RESULTS AND DISCUSSION

Introduction

The purpose of this work was to investigate the possibility of using differential reflectometry to identify and study thin film corrosion products on metal substrates. For this initial investigation, copper was chosen as the base metal because it has easily formed thin film corrosion products which are visible to the eye. This ensures that there are optical transitions which would be detected by the differential reflectometer, since the instrument can examine a wavelength range greater than that visible to the eye. In addition, work had previously been performed here on copper alloys using the differential reflectometer, so the mechanics of preparing samples were known as well as the theory of interband transitions in copper and their relation to peaks in differential reflectograms.[51]

Both the theoretical or equilibrium (Figure 12A)[52] and experimental (Figure 12B)[53] Pourbaix diagrams are available for copper in nil chloride solutions. In the basic half of the diagram (pH 7-14) three species are

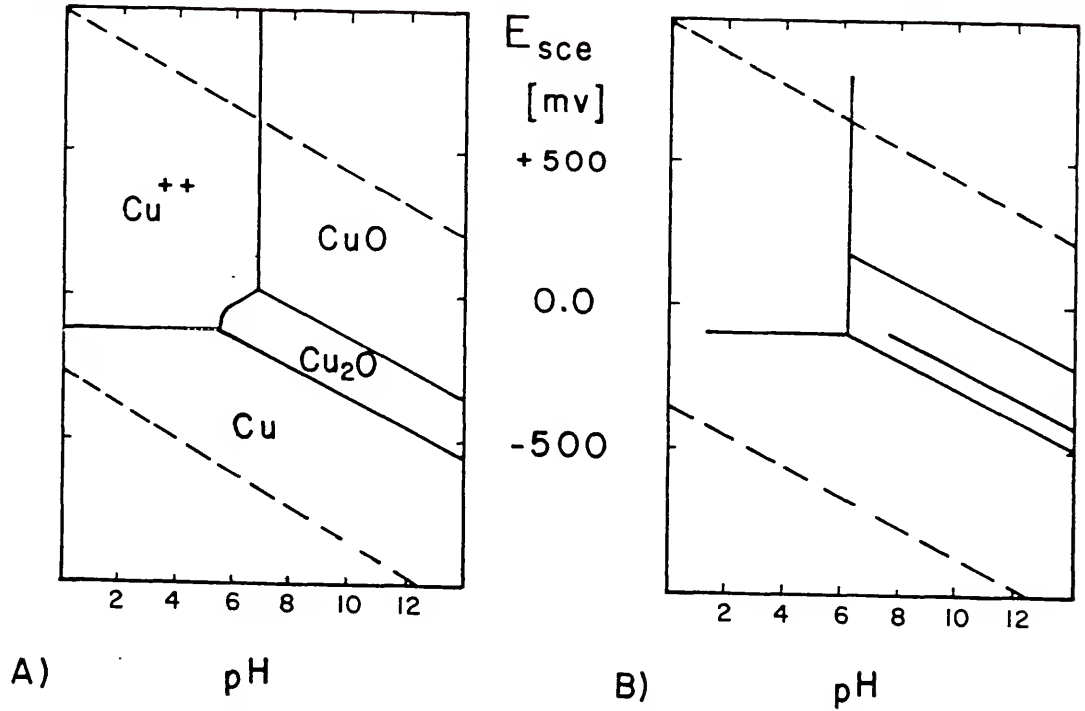

Figure 12. Theoretical (Figure 12A)[52] and experimental (Figure 12B)[53] Pourbaix diagrams for copper in nil chloride solutions.

shown to be stable depending upon the potential: copper; cuprous oxide (Cu_2O); and, cupric oxide (CuO). Typical differential reflectograms, which will be explained in detail later in this section, are shown in Figures 13 and 14. Figure 13 shows a differential reflectogram of a sample prepared in the Cu_2O region of the Pourbaix diagram (sixty-six hours at pH 9.2, -225 mv SCE). Figure 14 is a typical curve obtained from a specimen prepared in the CuO region of the Pourbaix diagram (eighteen hours at pH 9.2, +200 mv SCE). The structures are quite different and easily distinguished. By way of comparison, a typical compositional modulation differential reflectogram of a copper versus copper/1 at.% aluminum alloy is shown in Figure 15. Composition modulation spectra are not at all similar to the differential reflectograms of thin film corrosion products and are therefore easily differentiated from them.

Theory of Differential Reflectograms of Thin Films

Thermodynamic predictions and x-ray analysis are two methods by which differential reflectograms of thin films might be associated with particular corrosion products. Another method is to predict the particular differential reflectogram a given film would produce. In order to

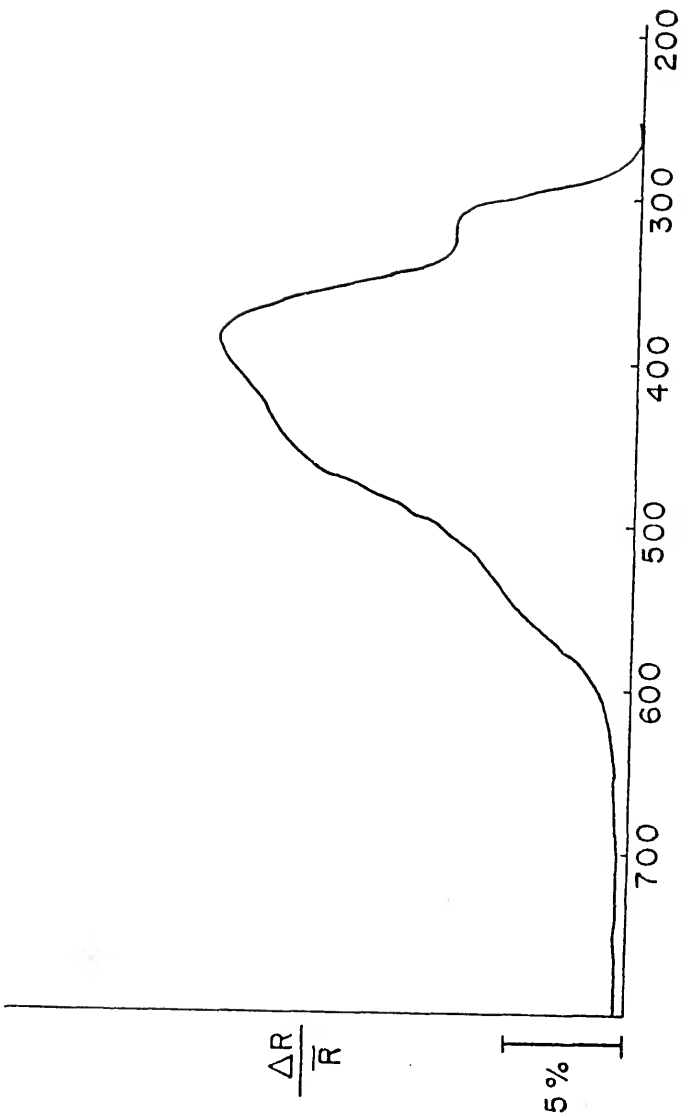

Figure 13. Differential reflectogram of a sample prepared in the Cu_2O region of the Pourbaix diagram (-225 mv SCE, pH 9.2, 66 hours).

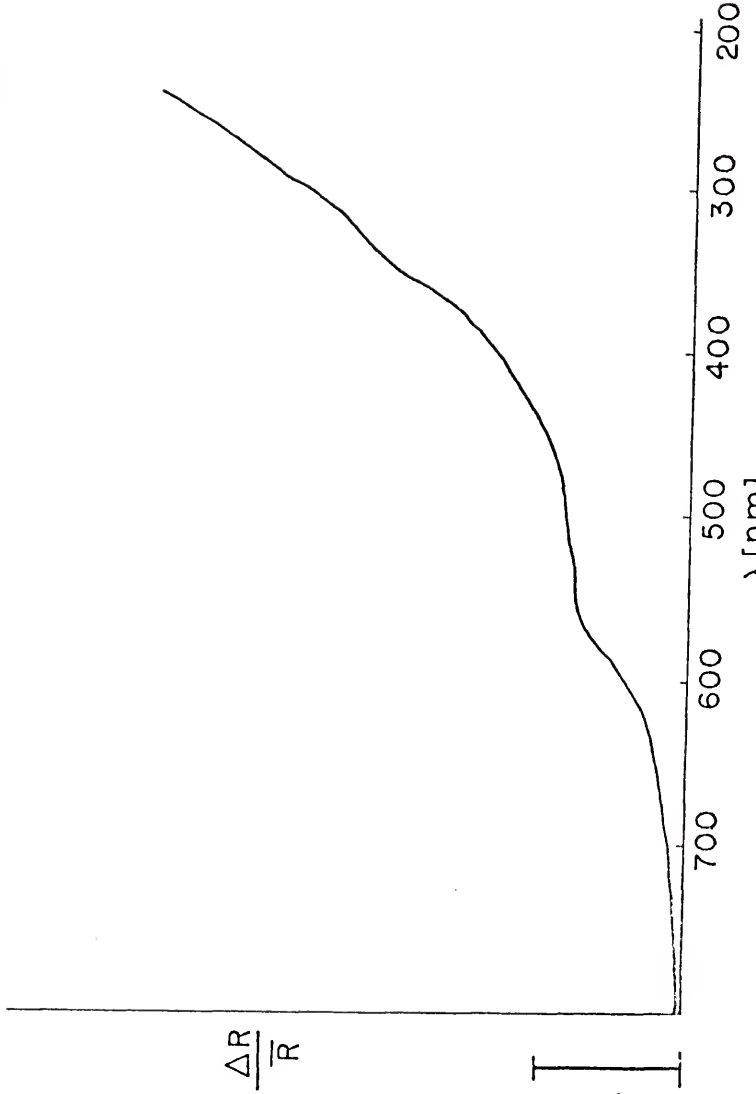

Figure 14. Differential reflectogram of a sample prepared in the CuO region of the Pourbaix diagram (+200 mv SCE, pH 9.2, 18 hours).

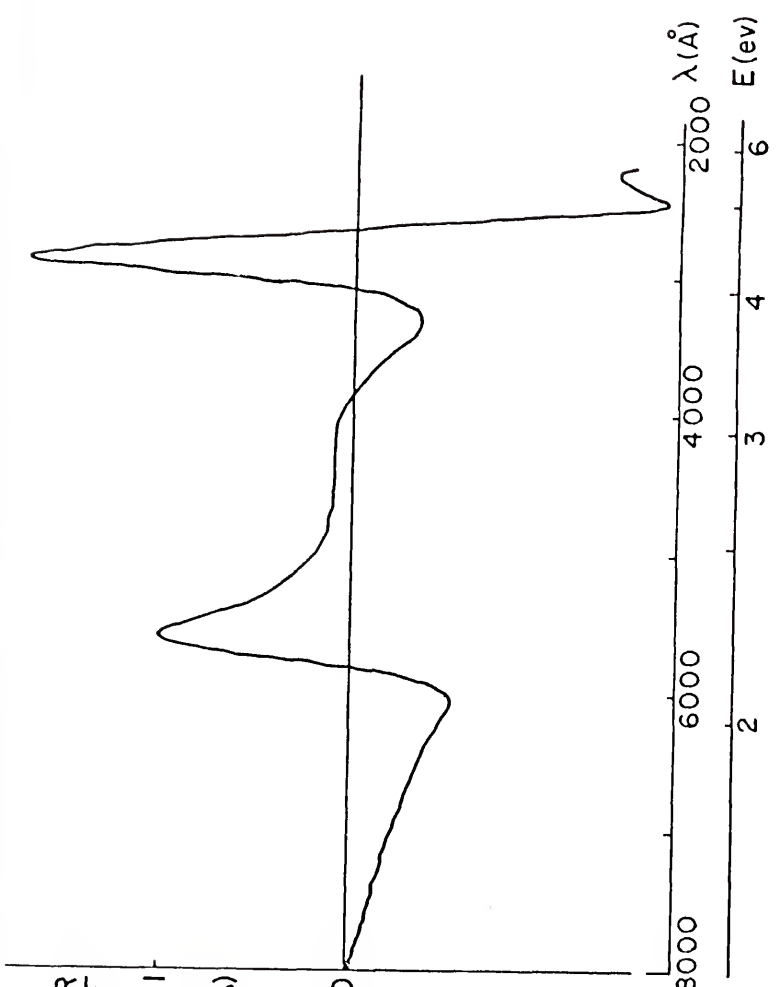

Figure 15. Typical compositional modulation differential reflectogram. One sample is pure copper, the other copper with 1 at.% aluminum in solid solution.[48,49]

perform these calculations, the index of refraction, n, and the index of absorption, k, for both the film and the metal substrate must be known as a function of wavelength.

The equations necessary to calculate the reflectivity of the film covered metal surface have been described by Heavens.[7] Referring to Figure 16, n_0 is the index of refraction of the medium surrounding the sample, which here is either air ($n_0 = 1.00$) or electrolyte ($n_0 = 1.33$). The thin film corrosion product has optical constants n_1 and k_1, and the thickness d, while the metal substrate has optical constants n_2 and k_2. We have, then,

$$g_1 \equiv \frac{n_0^2 - n_1^2 - k_1^2}{(n_0+n_1)^2 + k_1^2} \qquad h_1 \equiv \frac{2n_0k_1}{(n_0+n_1)^2 + k_1^2}$$

$$g_2 \equiv \frac{n_1^2 - n_2^2 + k_1^2 - k_2^2}{(n_1+n_2)^2 + (k_1+k_2)^2} \qquad h_2 \equiv \frac{2(n_1k_2 - n_2k_1)}{(n_1+n_2)^2 + (k_1+k_2)^2}$$

$$\alpha = \frac{2\pi k_1 d}{\lambda}[\text{radians}] \qquad \gamma = \frac{2\pi n_1 d}{\lambda}[\text{radians}]$$

The reflectivity, R_2, of the film/metal surface is

$$R_2 = \frac{(g_1^2+h_1^2)e^{-2\alpha} + (g_2^2+h_2^2)e^{2\alpha} + A\cos 2\gamma + B\sin 2\gamma}{e^{2\alpha} + (g_1^2+h_1^2)(g_2^2+h_2^2)e^{-2\alpha} + C\cos 2\gamma + D\sin 2\gamma} \qquad (4)$$

where

$$A = 2(g_1g_2 + h_1h_2) \qquad B = 2(g_1h_2 - g_2h_1)$$

$$C = 2(g_1g_2 - h_1h_2) \qquad D = 2(g_1h_2 + g_2h_1)$$

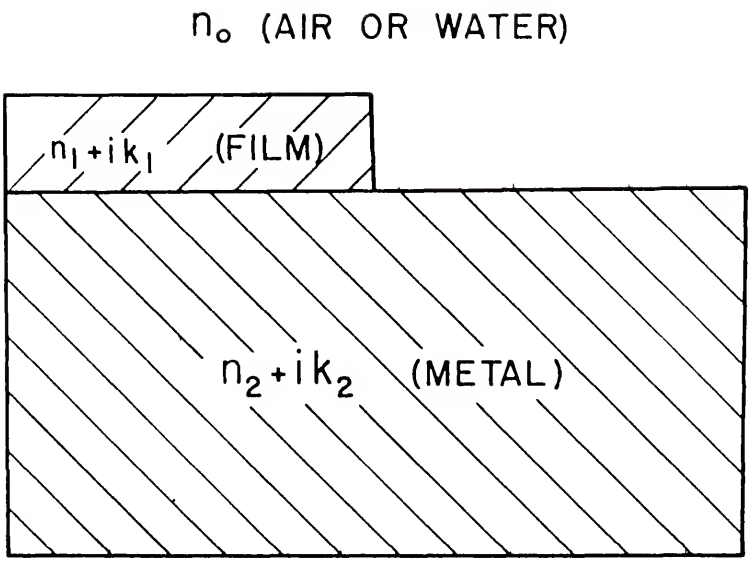

Figure 16. Schematic representation of a typical sample, with an oxide film covering half the exposed surface.

The reflectivity of the clean copper surface is much easier to calculate. Calling R_1 the reflectivity of the copper surface and using the same notation for the optical constants,

$$R_1 = \frac{(n_2-n_0)^2+k_2^2}{(n_2+n_0)^2+k_2^2} \tag{5}$$

The normalized difference in reflectivity is easily obtained:

$$\frac{\Delta R}{\bar{R}} = \frac{R_1-R_2}{(\frac{R_1+R_2}{2})} \tag{6}$$

These equations should reproduce the experimental differential reflectograms for non-*in situ* experiments if $n_0 = 1.00$ and if values of n and k are available in the literature for copper and its oxide as a function of wavelength. In addition, if the effect of collodion is neglected, it should be possible to reproduce differential reflectograms of *in situ* experiments. In this case, $n_0 = 1.33$, the index of refraction of water, which is approximately that of the electrolyte.

These calculations have been performed for the case of a cupric oxide (CuO) film since the optical constants for that compound have been published as a function of wavelength.[6] The optical constants for copper which were

used in these calculations are those of Schultz and Tangherlini[54,55] and are given in Table 4.

Figure 17 is the plot of the variation in $\Delta R/\overline{R}$ for CuO film on copper substrates as a function of film thickness for a fixed wavelength of light. The particular wavelength used in these calculations was 600 nm, but the curve is similar to those calculated for other wavelengths. The curve shows a large increase in the differential reflectivity for the first few hundred angstroms of film thickness, followed by strong oscillations which are gradually damped out. The oscillations are caused by interference effects which occur when the film thickness is of the same order of magnitude as the wavelength of the incoming light. For constructive interference in this case, the film thickness must be[56]

$$d = \frac{m\lambda}{2n_1} \tag{7}$$

where n_1 is the index of refraction of the film, as before, and m is the order of the interference. The damping effect is due to the fact that as the film thickness, d, increases, less light penetrates to the underlying metal surface. The reflectivity of the film/metal surface slowly approaches the reflectivity of a bulk specimen with the composition of the film. Further increases in the

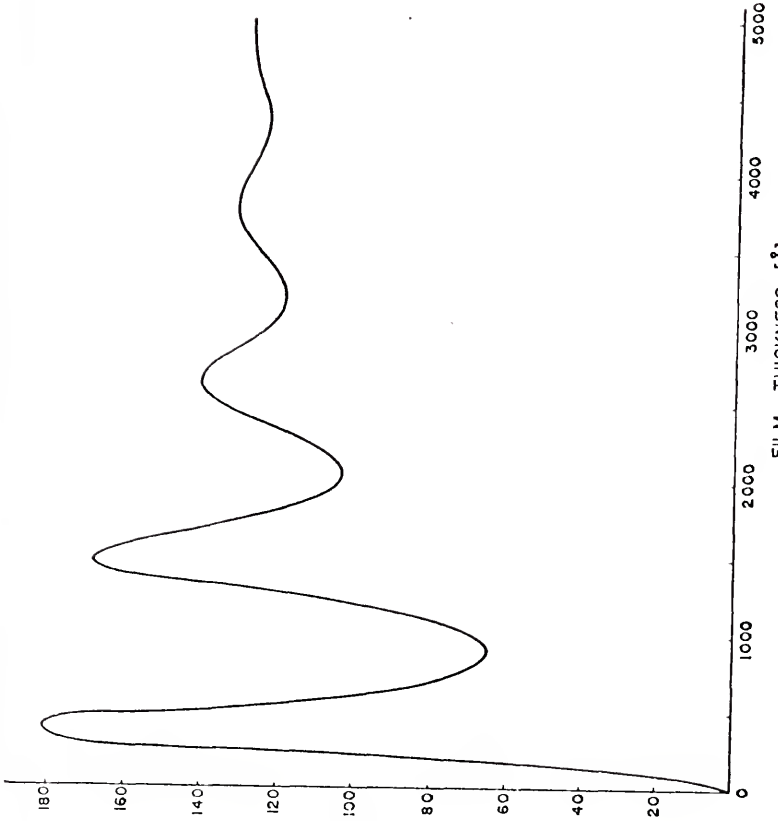

Figure 17. Variation in $\Delta R/\bar{R}$ as a function of film thickness for a CuO film on a copper substrate. The wavelength of light used is assumed to be 600 nm.

Table 4

Optical Constants $\hat{n} = n+ik$ for Copper and Cupric Oxide (CuO) as a Function of Wavelength[6,54,55]

λ [nm]	Copper		CuO	
	n	k	n	k
450	.87	2.20	2.45	.744
500	.88	2.42	2.59	.650
550	.72	2.42	2.57	.539
600	.17	3.07	2.60	.449
650	.13	3.65	2.65	.345
700	.12	4.17	2.64	.236
750	.12	4.62	2.65	.170
800	.12	5.07	2.62	.132

thickness of the film do not change the reflectivity. Since the clean copper surface has a constant reflectivity at a given wavelength, the differential reflectivity does not change after the film reaches a certain minimum thickness. For the case of the CuO film this occurs at roughly 7500 Å, beyond which the differential reflectivity is a constant 127%.

Other wavelengths of incident light show similar oscillations with slightly different periodicity. This interference can produce peaks in differential reflectograms which are not due to interband transitions but rather are due to the thickness and index of refraction of the film. As a result, differential reflectometer spectra of thin films on metal substrates can have structure which varies as the film thickness changes. For example, Figure 18 shows the theoretically calculated differential reflectogram for a CuO film of 100 Å thickness. Two curves are shown, one for which the medium surrounding the sample is air ($n_0 = 1.00$) and one for which the surrounding medium is assumed to be electrolyte ($n_0 = 1.33$). Both curves are essentially the same, indicating that there should be little difference between spectra taken *in situ* or non-*in situ* if the effect of collodion is neglected. These curves differ slightly from

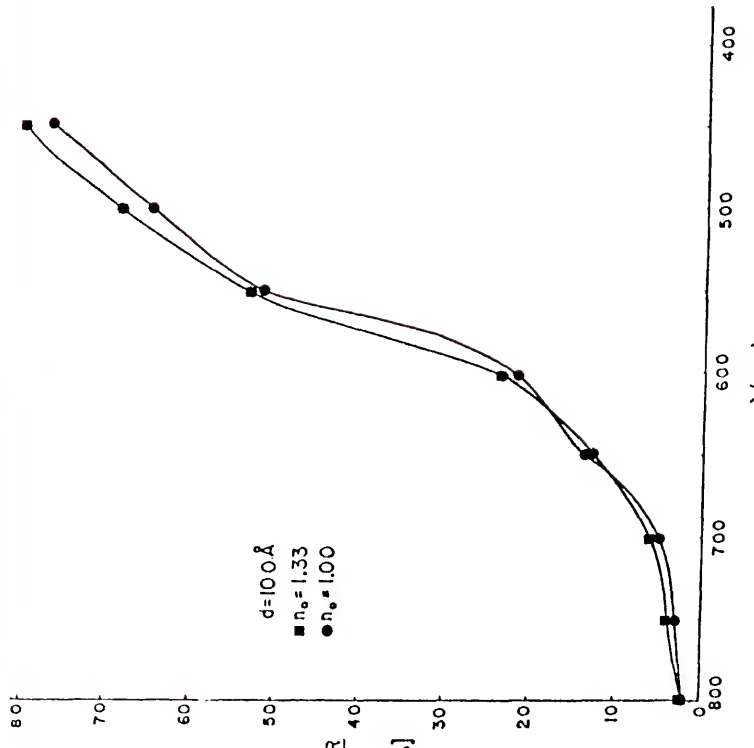

Figure 18. Theoretically constructed differential reflectogram of a CuO film 100 Å thick on a copper substrate. λ = 600 nm.

the theoretical curve calculated for a 35 Å thick CuO film in air (Figure 19) but are significantly different compared to the spectra of a 500 Å film (Figure 20). Finally, Figure 21 shows the calculated differential reflectograms for a 7500 Å CuO film surrounded by air or by an electrolyte. Film thicknesses greater than 7500 Å should produce spectra similar to Figure 21, since in this case the light beam will not be able to penetrate the film all the way to the film/metal interface. As can be seen by comparing Figure 21 with Figure 19, such curves bear no resemblance to those of very thin films. Fortunately, as will be described below, the thin film corrosion products which were generated in this work have a thickness which appears to be significantly smaller than the critical thickness at which interference effects begin to distort the differential reflectograms.

Using Equation 7 with $n_1 = 2.1$ and $\lambda = 2500$ Å, the first interference maximum is at about $d = 600$ Å. Wavelengths greater than 2500 Å (which is the wavelength where most differential reflectograms begin) place the first maxima at higher thicknesses. Therefore for thicknesses up to at least 200 Å the differential reflectogram should

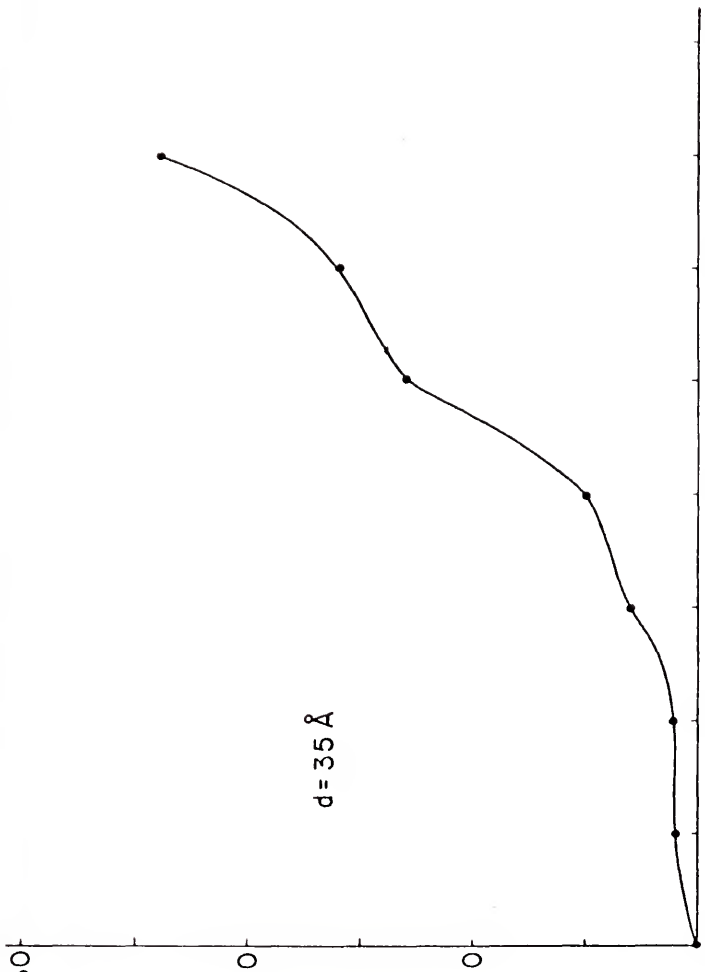

Figure 19. Theoretically constructed differential reflectogram of a CuO film 35 Å thick on a copper substrate. λ = 600 nm.

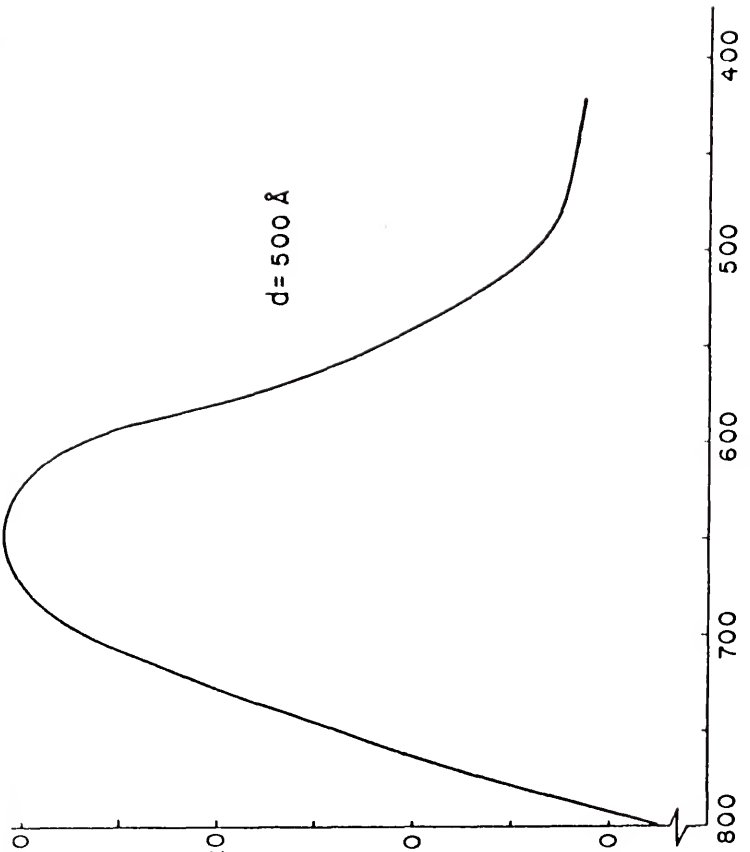

Figure 20. Theoretically constructed differential reflectogram of a CuO film 500 Å thick on a copper substrate. λ = 600 nm.

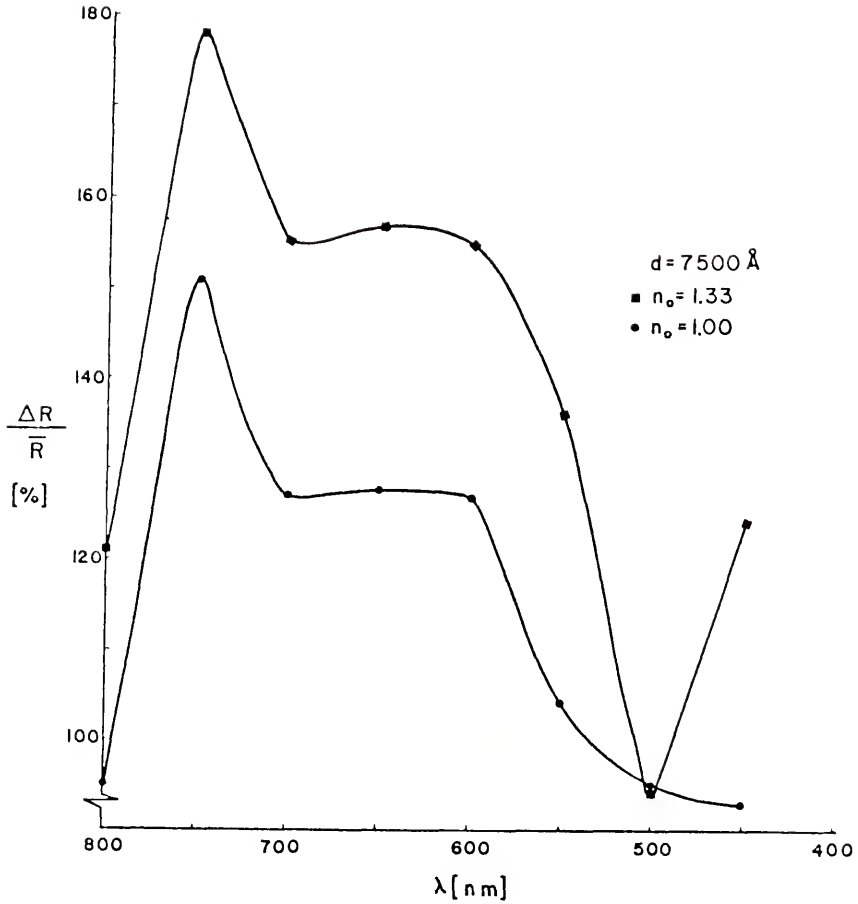

Figure 21. Theoretically constructed differential reflectogram of a CuO film 7500 Å thick on a copper substrate. λ = 600 nm.

not show an appreciable effect from interference. Film thicknesses greater than 7500 Å should also be free of interference effects, since the light beam should not reach the copper substrate under the corrosion product film. Thus there may be defined three distinct ranges relating film thickness to differential reflectometry. In the first range, where film thicknesses range from 0 to at least 200 Å, the structure in a differential reflectogram is constant and unique for each kind of film. The thickness of the film determines the intensity of the differential reflectivity. In the second range, extending to a thickness of about 7500 Å, interference effects dominate the spectra. Finally, in the third range, where the film thickness is greater than 7500 Å, the differential reflectogram will again be unique for each corrosion product. However, peak intensities will be constant and unaffected by increasing film thickness.

The differential reflectometer should be most useful in the first range, where intensity is related to film thickness. Figure 22 shows the variation in $\Delta R/\overline{R}$ with film thickness for the same conditions as Figure 17 (CuO film, copper substrate and reference, $n_0 = 1.00$), but over the more restricted film thickness range d = 0 to 200 Å. This curve may be fitted to either a power curve,

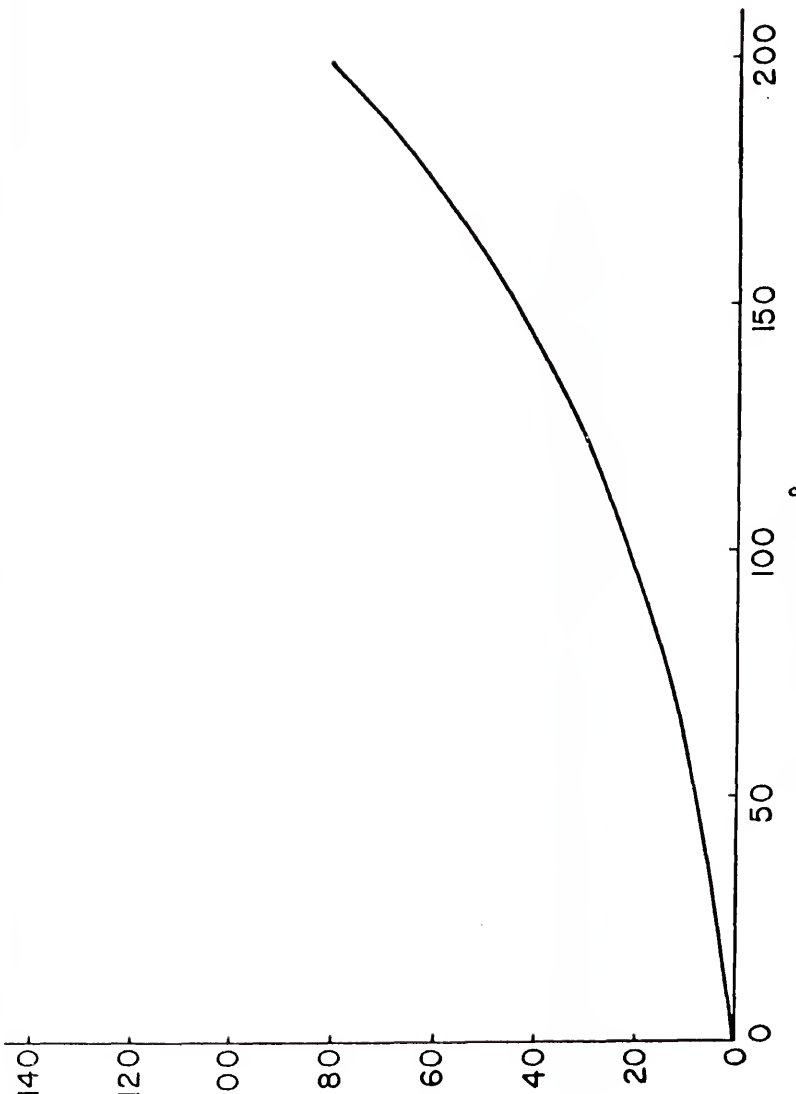

Figure 22. Variation in $\Delta R/\bar{R}$ as a function of film thickness for a CuO film on a copper substrate over the range d = 0 to 200 Å. The wavelength of light is assumed to be 600 nm.

$\Delta R/\overline{R} = .03d^{1.45}$, or an exponential curve, $\Delta R/\overline{R} = 2.45e^{.02d}$, with correlation coefficients .99 and .92, respectively. The curve is sufficiently steep that an uncertainty in $\Delta R/\overline{R}$ of 5%, which is extremely conservative, produces an uncertainty in the film thickness of only 5 Å. This thickness is on the order of a monolayer of atoms.

Figure 23 shows an experimentally obtained differential reflectogram of a sample potentiostated in the CuO region of the Pourbaix diagram (+500 mv SCE, pH 9.2, eighteen hours) and a theoretically calculated differential reflectogram of a sample covered with a CuO film 25 Å thick. The agreement is quite reasonable. The differences which do exist can probably be attributed to the fact that the optical constants of very thin films are seldom precisely the same as those of thicker films or bulk samples. The data of Ladelfe, Czanderna, and Biegen,[6] which were used here, were obtained from transmittance measurements on films between 350 Å and 1800 Å in thickness prepared by the thermal oxidation of copper. Such films would tend to have optical constants more nearly like bulk CuO, whereas electrochemically prepared thin films would tend to have gradients in the optical constants. The optical constants of the film would be

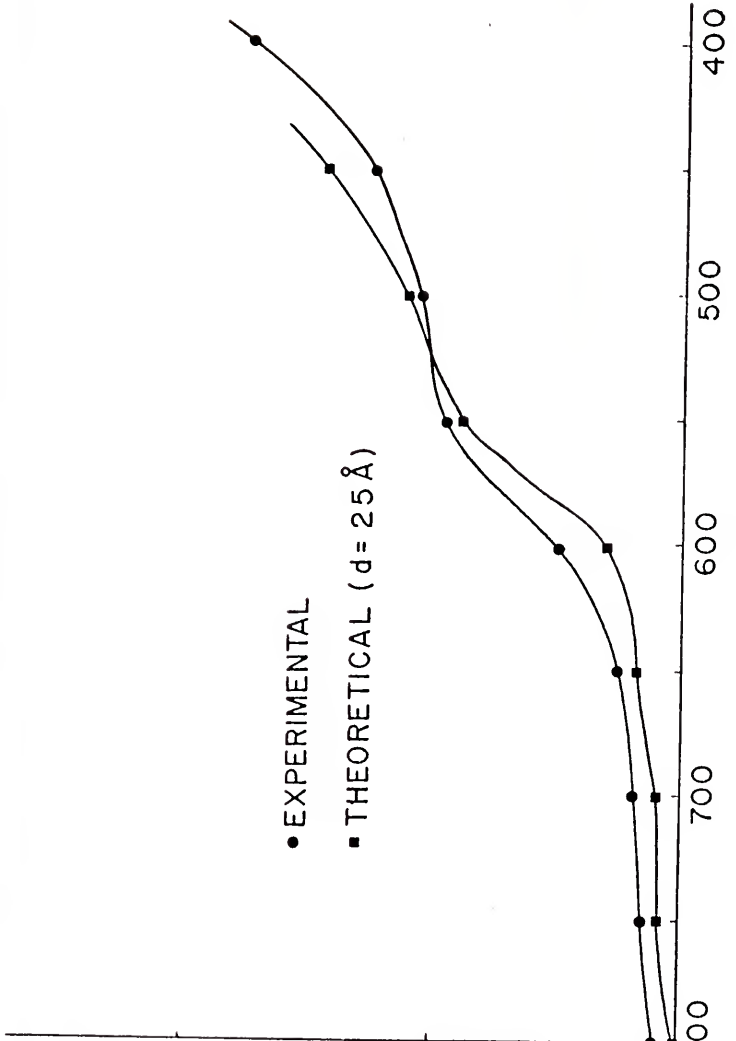

Figure 23. Comparison of the differential reflectogram of an experimentally prepared CuO film (potentiostated at +500 mv SCE at pH 9.2 for 18 hours) to a theoretically constructed reflectogram of a CuO film 25 Å thick.

more like those of copper at the copper/film interface, and more like those of bulk CuO at the film/electrolyte interface. As a result, calculated differential reflectograms prepared from the optical constants of thermally grown compounds should not be expected to exactly match the differential reflectograms of electrochemically prepared compounds.

A CuO film 25 Å thick may seem surprisingly thin, but films near this thickness are necessary to give good agreement between the experimentally observed and the theoretically calculated differential reflectograms. In addition, Kruger[45] observed CuO and Cu_2O film thicknesses on the order of 100 Å or less for films grown in air or water. In addition, measurements were performed on several films using an interferometric microscope.* Precise measurements of film thicknesses less than 100 Å are not possible with this instrument, so an exact measurement of the film thickness was not obtained. However, the instrument did unambiguously indicate a film thickness of less than 100 Å for each film measured. In order to be observed with the interferometric microscope

*Model M-111 Angstrommeter, Sloan Instrument Co., Santa Clara, California

the film must be overcoated with a thin layer of evaporated aluminum or other metal. This involves placing the sample in a vacuum which could conceivably have altered the film, producing inaccurate measurements of the thickness. For this reason measurements with an interferometric microscope are not entirely reliable for corrosion applications.

Finally, a working ellipsometer has become available recently at the University of Florida. Measurements of a typical CuO film, prepared by potentiostating in a nil chloride solution of pH 9.2 for eighteen hours at +100 mv SCE, indicate a film thickness of about 45 Å. All these measurements point to film thicknesses for typical specimens of well less than 200 Å. In this thickness range, the peak positions in the differential reflectograms remain essentially constant, and the peak intensities may be used to calculate the film thicknesses to a high degree of precision.

Non-*In Situ* Experiments

In this section the results of experiments which were not performed in the *in situ* cell will be discussed. Longer exposures to the electrolyte are possible using this method than in true *in situ* studies because of the

tendency of the protective collodion film, used in *in situ* experiments to cover the copper reference side of the sample, to break down after a certain amount of time in the electrolyte. The disadvantage is that changes in some films are possible between the time of removal of the sample from the electrolyte and the measurement of the differential reflectogram. Three types of film formation were studied: films formed in air; films formed in distilled water; and, films formed in electrolyte solutions during potentiostating.

Films formed during exposure to the atmosphere were prepared by the simple technique of covering half the sample with a protective layer of Miccroflex and permitting the sample to remain exposed to the atmosphere. An inverted beaker or glass plate was used to prevent dust from settling on the specimen. Similar experiments were performed with samples exposed to an atmosphere of pure oxygen. In these cases the sample was placed in an airtight dessicator which was repeatedly flushed with oxygen.

The results of the experiments where the sample was exposed to the uncontrolled atmosphere were seldom completely reproducible. Greater or lesser amounts of various oxides could be formed depending on the initial

conditions, length of exposure time, and relative humidity. As a result, between ten and twenty runs were made for each variation in the experiment, under conditions which were kept as identical as possible, in order to determine trends of film formation. Normally approximately 80% of the runs produced essentially identical results.

Samples exposed to a normal indoor atmosphere for a moderate period of time (one to three days) yielded differential reflectograms essentially the same as Figure 13; that is, indicative of cuprous oxide, Cu_2O. Other samples exposed to air for longer times (five to fourteen days) tended to produce CuO patterns, as did all the samples exposed to a pure oxygen atmosphere. Kruger[45] has pointed out that Cu_2O is the oxide produced upon initial exposure of copper to an uncontrolled atmosphere. However, the Cu-O phase diagram[57] predicts that CuO is the stable species if copper is exposed to dry air below 375°C. This apparent inconsistency can probably be explained by the fact that the normal Florida atmosphere is not at all dry. Water vapor probably induces the formation of Cu_2O rather than CuO. In addition, CuO tends to be reduced to Cu_2O in the presence of metallic copper, so it is likely that there is at least a monolayer of Cu_2O at the interface between Cu_2O and Cu. Hence copper exposed to the

atmosphere for a brief period of time may well show more of a Cu_2O pattern than a CuO pattern. Presumably exposure to the atmosphere for longer times or exposure to pure, dry oxygen would favor the growth of the equilibrium oxide, CuO, as was observed.

In order to study the films formed in distilled water, samples were prepared in the usual manner, partially covered with Miccroflex, and immersed in a beaker containing approximately 500 ml of triply distilled water. A magnetic stirrer was used to maintain circulation. In some cases the water was simply exposed to the atmosphere; in others oxygen was bubbled through the water at a rate of about 10 cc/sec.

Samples placed in distilled water which was exposed to the atmosphere usually produced differential reflectograms indicative of mixed oxides (CuO and Cu_2O) with the Cu_2O being predominant. In a few cases only Cu_2O was apparent. This is in agreement with the work of Kruger,[45] who also found Cu_2O films. Kruger[45] has also noted that the Pourbaix diagram predicts the formation of CuO, rather than Cu_2O, under these conditions.

One of the advantages of the differential reflectometer is its ability to clearly demonstrate the presence of mixed oxides, such as are found in the above experi-

ment. The results seem to show a simple addition of the spectrum of one compound to the spectrum of the other. In the case of samples placed in distilled water through which oxygen was continuously bubbled, mixed oxides of Cu_2O and CuO were again produced. A typical result is shown in Figure 24, where the structure at 310, 330, and 380 nm is characteristic of Cu_2O (see Figure 13), and the rising tail visible below 300 nm is characteristic of CuO (see Figure 14). Although a quantitative analysis of such mixed oxides is not possible at this time due to a lack of information on the optical constants of the Cu_2O phase and to the increased mathematical complexities of multilayer reflection, such analyses are certainly possible in principle.

The most extensive studies to date have been in boric acid buffered electrolyte with samples potentiostated in some particular region of the Pourbaix diagram. For the most part these experiments agree well with the Pourbaix diagram determined experimentally by electrochemical techniques (Figure 12B). However, the differential reflectometer provides additional insight into the composition, thickness, and uniformity of the corrosion products.

An example of the additional information which may be obtained using optical techniques is shown in Fig-

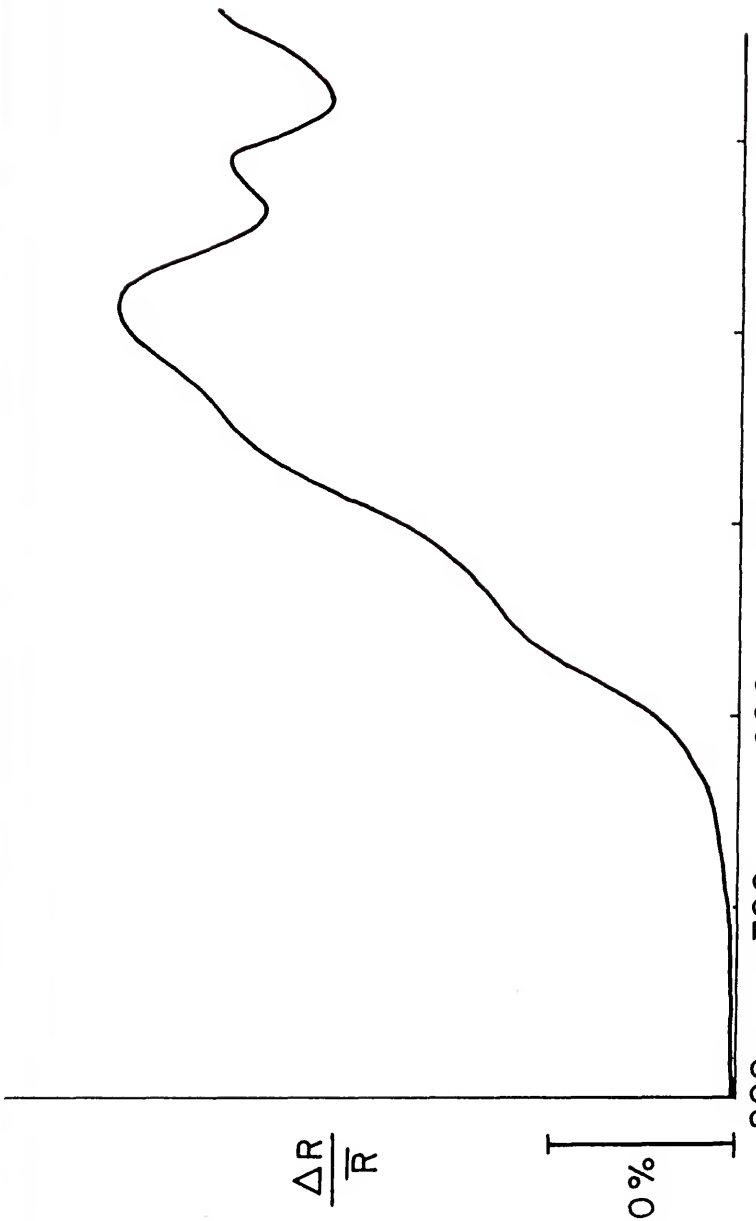

Figure 24. Differential reflectogram of a sample prepared by immersion in distilled water for eighteen hours, with a continuous stream of oxygen bubbled through the water. The structure is characteristic of a mixed oxide of Cu_2O and CuO.

ure 25, which shows a differential reflectogram of a sample potentiostated at -50 mv SCE and pH 9.2 for eighteen hours. Three scans are shown, taken at three different areas of the sample. Several points are readily apparent.

1) The thin film corrosion product is primarily Cu_2O, as indicated by the structure at 315, 330, and 380 nm.

2) The rising slope between 300 and 200 nm indicates a small amount of CuO present in the sample.

3) Variations in intensity indicate differences in film thickness, with the film thickness decreasing from position C to position A.

Mixed oxide films such as those indicated by the spectra of Figure 25 are not uncommon. This sample is typical of those potentiostated near the Cu_2O/CuO equilibrium line (-50 mv SCE at pH 9.2 is essentially on the equilibrium line). It illustrates the fact that in such regions of the Pourbaix diagram one corrosion product is not much more stable than the other. Initial conditions, such as the presence or absence of a spot of oxide, or a local homogeneity in the copper or electrolyte, may influence which corrosion product may form in any specific microscopic area. Samples potentiostated well into a

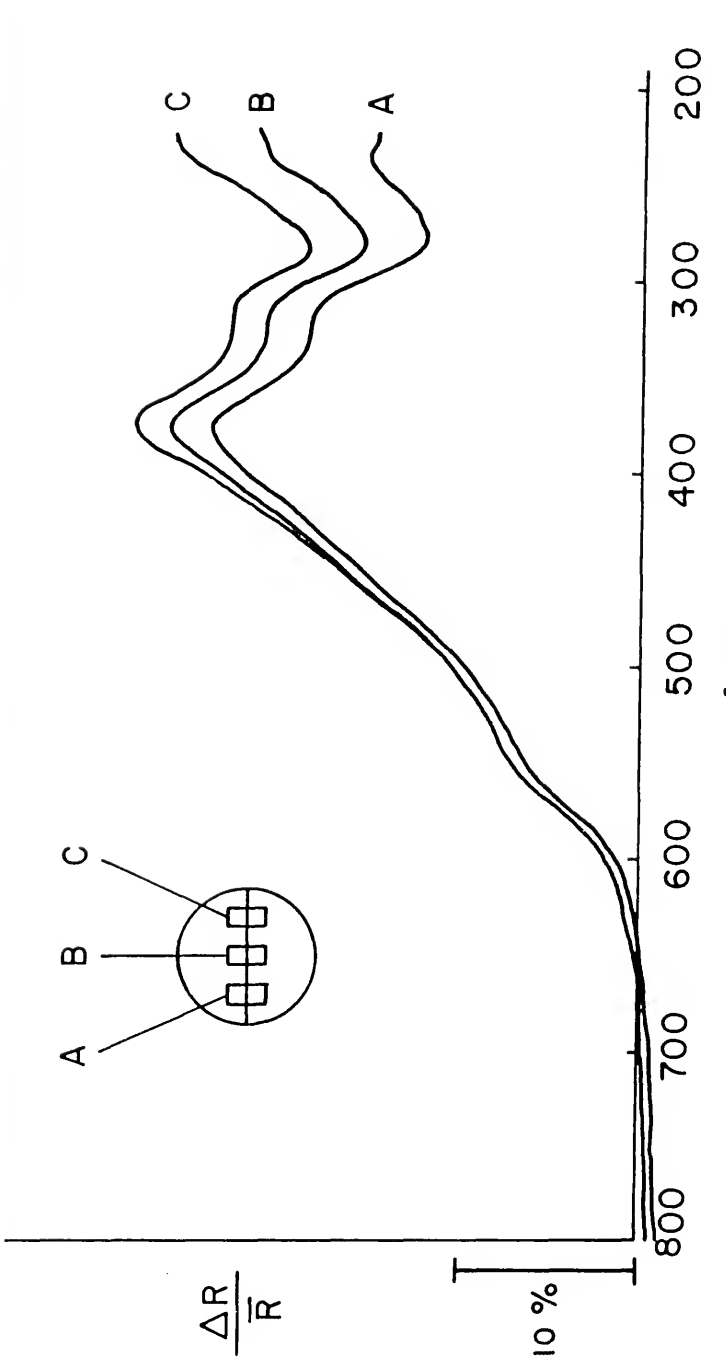

Figure 25. Differential reflectograms of three areas of the same sample, which had been potentiostated near the Cu_2O/CuO equilibrium line (-50 mv SCE at pH 9.2) for eighteen hours.

specific region of the Pourbaix diagram consistently show only the expected corrosion product, as in the case of the differential reflectograms shown in Figure 13 (-225 mv SCE, pH 9.2), which is typical of a pure Cu_2O film, and Figure 14 (+200 mv SCE, pH 9.2), which is typical of a CuO film.

A large amount of data was collected with the aim of defining more precisely the positions of the lines delineating the areas of stability of the experimental copper/nil chloride Pourbaix diagram. This is complicated by the fact that these lines are coexistance lines, so that both compounds are present near the boundaries, as confirmed by the differential reflectometer. Furthermore, the boundaries can be slightly time-dependent. For example, a sample potentiostated just into the CuO region of the Pourbaix diagram, but near the Cu_2O area, might show Cu_2O components in the structure of the differential reflectogram if the exposure time was brief. In this case the CuO which formed against the copper surface might be reduced when the potential was removed. Alternately, as was mentioned earlier, a thin layer of Cu_2O might always be present at the Cu/CuO interface, regardless of where in the Pourbaix diagram the experiment takes place. In this case, very thin (that is, short exposure time) CuO films

may show appreciable Cu_2O structure due to a monolayer of Cu_2O at the interface. In this regard, it should be re-emphasized that even a monolayer can produce significant changes in the differential reflectivity. In the case of CuO (see Figure 22), a change in thickness of a single monolayer (about 5 Å) can cause a change in the differential reflectivity of several percent. Such a change is very readily detected with the present instrument.

As a prelude to true *in situ* measurement of the differential reflectivity, certain experiments were undertaken to monitor changes in film properties with changing experimental conditions. Figure 26A shows a differential reflectogram of a copper sample potentiostated in a nil chloride solution of pH 10 at +500 mv SCE for sixteen hours. This potential is well into the CuO region of the Pourbaix diagram. The resulting spectra is similar to Figure 14, and is characteristic of CuO. After measurement, half of the sample which serves as a pure copper reference, was recoated with Miccroflex lacquer, and the sample immersed in fresh electrolyte. This time, however, the sample was potentiostated in the Cu_2O region of the Pourbaix diagram, at -225 mv SCE. After twenty hours the sample was removed and remeasured, producing the

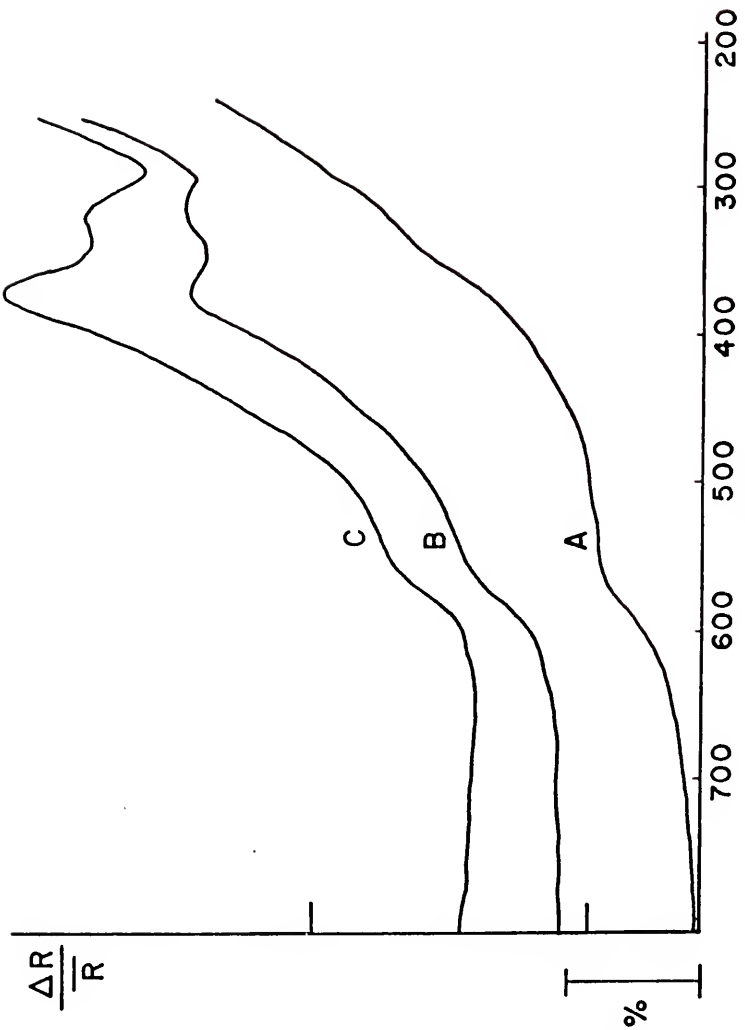

Figure 26. Differential reflectogram of a sample potentiostated in the CuO region (A) of the Pourbaix diagram, and of the same sample after the potential has been changed to the Cu_2O region (B). Curve C is the same sample potentiostated for a longer period of time in the Cu_2O region. The baselines of the curves have been shifted for clarity.

spectra of Figure 26B. New structure, characteristic of Cu_2O, is evident at 320 and 380 nm, superimposed on the strong CuO background. The clean copper side of the sample was again recoated, and the sample again potentiostated at -225 mv for an additional sixty-eight hours. When the sample was measured for the third time, the curve of Figure 26C was produced, showing clear evidence of extensive Cu_2O film formation. The peak positions and even their relative intensities are characteristic of Cu_2O.

The differential reflectometer yields other information on the films formed in Figure 26 in addition to their identity. The zero lines of Figure 26 have been shifted for clarity, but a superposition of the three curves indicates that the CuO pattern remains relatively constant, while the Cu_2O pattern "grows" on top of it. Since the intensity of the CuO structure is directly proportional to the thickness of the film (see Figure 22), it is reasonable to assume that the thickness of the CuO film does not change substantially when the potential is shifted to the Cu_2O area of the Pourbaix diagram. Hence, the shift in potential induces growth of a Cu_2O layer under the existing CuO layer, rather than the dissolution of the CuO layer. This is significant observation which could

not be readily obtained with strictly electrochemical techniques.

In Situ Experiments

One of the major advantages of the differential reflectometer compared to other techniques is its ability to perform *in situ* measurements. Theoretical considerations, explained in the experimental procedures section, indicate that an electrolyte surrounding the sample and the presence of a window to the corrosion cell should not introduce additional structure to the differential reflectogram. Figure 27 shows two differential reflectograms of samples potentiostated in the Cu_2O region of the Pourbaix diagram (-200 mv SCE, pH 9.2) for five and one-half hours. One is the spectrum of a sample prepared in the normal manner, where Miccroflex covered half the specimen surface. The other represents a sample prepared in collodion covering half the specimen surface and analyzed *in situ*. The sensitivity, or amount of amplification, for the two curves is identical. Three points stand out.

1) The peak positions of each curve are at the same wavelengths.

2) There is no additional structure introduced in the *in situ* spectrum.

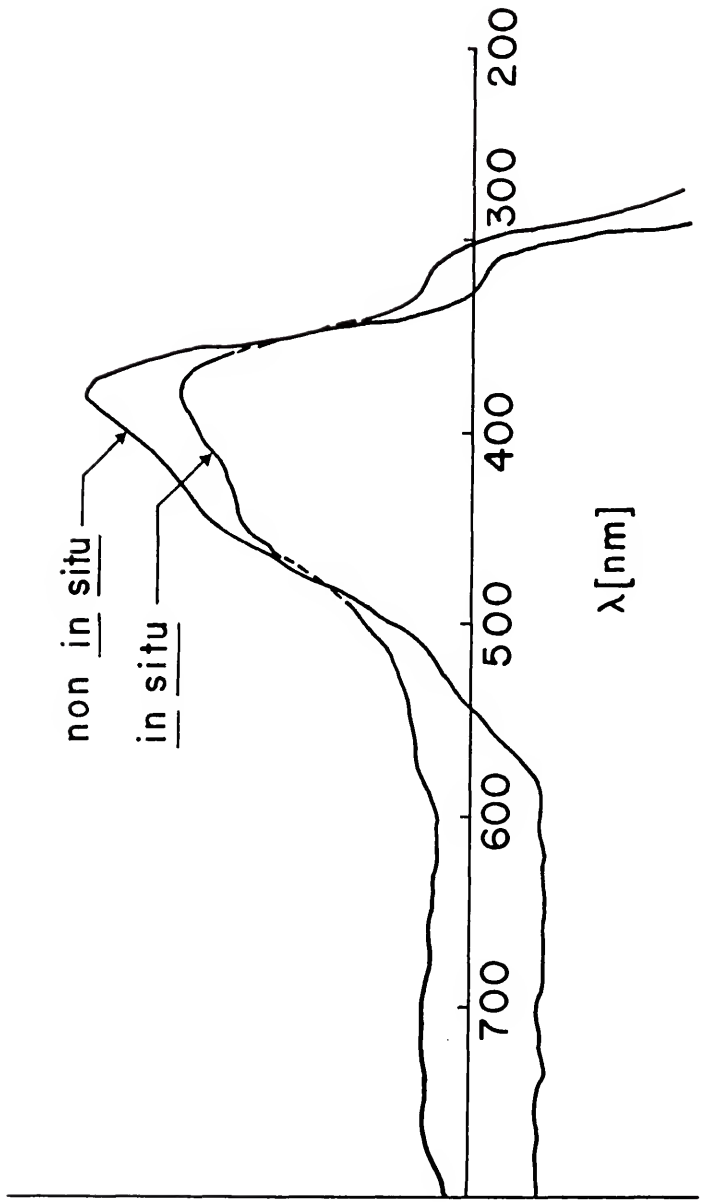

Figure 27. Differential reflectograms of two samples potentiostated under the same conditions (5.5 hours at -200 mv SCE, pH 9.2). The first was run in the non-*in situ* cell and measured in air, while the second was prepared and run *in situ*.

3) There is some loss of intensity or amplitude of the *in situ* curve compared to the non-*in situ* curve, and an associated increase in the noise level.

The first two points are most important because they establish the fact that this technique of making measurements gives results which are consistent with simpler measurements not performed *in situ*. The third point indicates that absorption of the light as it passes through the window, electrolyte, and collodion, as well as losses due to reflection at the air/window and window/electrolyte interface and small amounts of turbulence in the electrolyte, combine to produce a somewhat less intense and more noisy signal. This effect is not unexpected, nor is it troublesome as long as no additional structure is introduced in the differential reflectogram.

The spectra of Figure 27 were made after only five and one-half hours in order to minimize the degradation of the collodion coating on the *in situ* sample. In order to investigate the effect of the collodion on the intensity of the spectra, an additional experiment was performed. First, a sample was prepared in the usual manner in the Cu_2O region of the Pourbaix diagram. The sample was removed from the electrolyte, dried, and the Miccroflex stripped off. Figure 28A represents the differential

reflectogram made from this sample. The sample was placed in the dry *in situ* corrosion cell and another reflectogram made, Figure 28B. The lack of significant changes in the spectrum shows that the effect of the presence of the window is negligible. (The zero lines of Figures 28A and 28C have been shifted for clarity.) Next the *in situ* cell was filled with electrolyte and a third differential reflectogram taken immediately, before the thin film corrosion product could be altered to any great extent. This spectrum is shown in Figure 28C, which shows how an *in situ* differential reflectogram would appear if there were no collodion present on the "pure" copper side of the specimen. Compared to Figures 28A and 28B, there is a general sharpening of the peaks and an increase in intensity. These changes can be attributed to the coupling effect of the electrolyte, which acts as a light pipe to optically couple the window and sample more efficiently than when the sample is surrounded by air. The index of reflection of the corrosion product and the quartz window is more nearly matched by the index of refraction of the electrolyte than that of air, resulting in a more efficient optical coupling of the two surfaces. A similar effect is used in oil immersion optics. Here it partly compensates for the absorption of the light beam by the

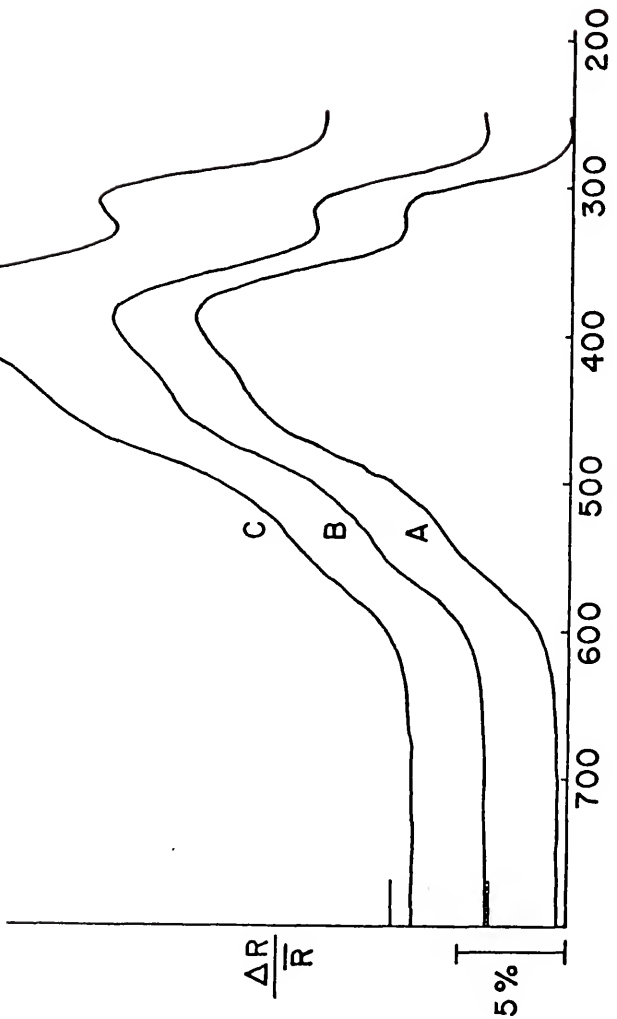

Figure 28. Differential reflectograms of a sample half covered with a Cu_2O film, showing the sample as measured in air (A), in the empty *in situ* cell (B), and in the *in situ* cell filled with electrolyte (C).

collodion. Without this coupling effect, uniform absorption of the light by the collodion would decrease the intensity of *in situ* measurements relative to non-*in situ* measurements more than is indicated by Figure 27.

Several experiments have been performed to monitor the growth of corrosion films *in situ*. One example is shown in Figures 29 and 30 which represent the evolution with time of the differential reflectograms of a sample potentiostated in the Cu_2O region of the Pourbaix diagram at pH 9.2 and a potential of -200 mv SCE. These curves are typical for samples potentiostated under these conditions, although in this case the collodion covering the "clean" copper resisted breakdown by the electrolyte for an unusually long time. Immediately after immersion (t = 0), the differential reflectogram shows a reasonably flat spectrum, with no evidence of structure. The displacement from the zero line actually decreases during the first three hours after immersion, perhaps showing the dissolution of a previously formed oxide. It is also possible that the decrease in intensity is due to interference effects discussed in the theoretical section. This was probably not the case, however, since no further oscillations were observed. In addition, interference oscillations would imply a film thickness of over 500 Å,

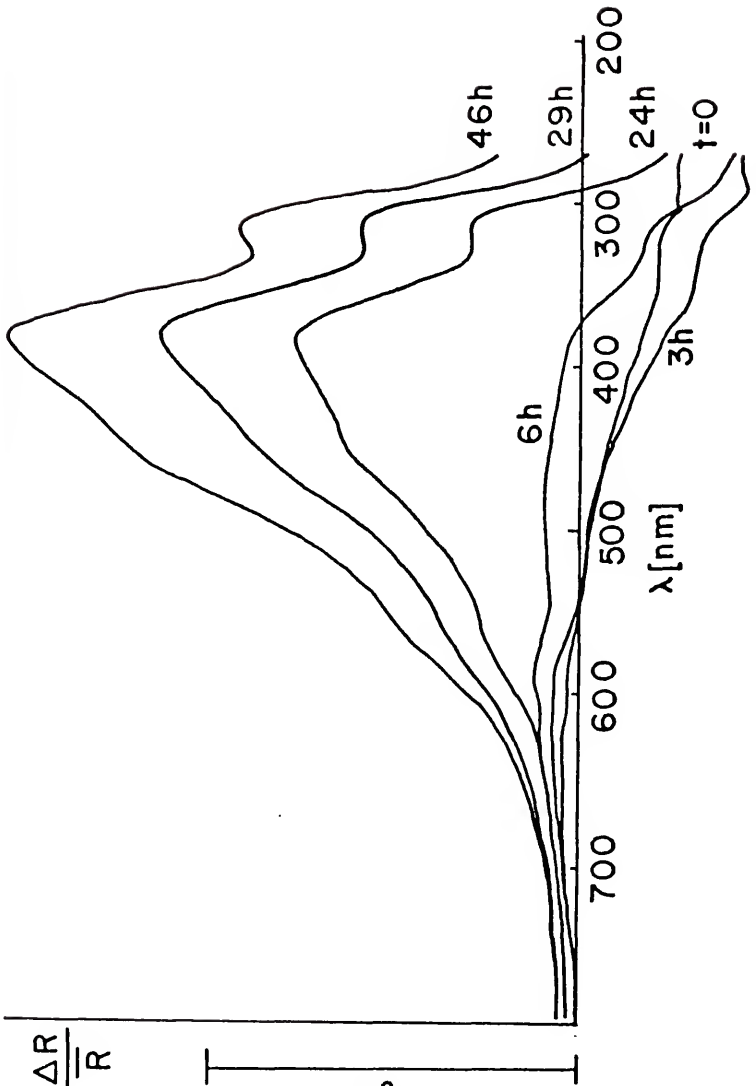

Figure 29. *In situ* differential reflectograms of a copper sample potentiostated at -200 mv SCE, pH 9.2, which is in the Cu_2O region of the Pourbaix diagram.

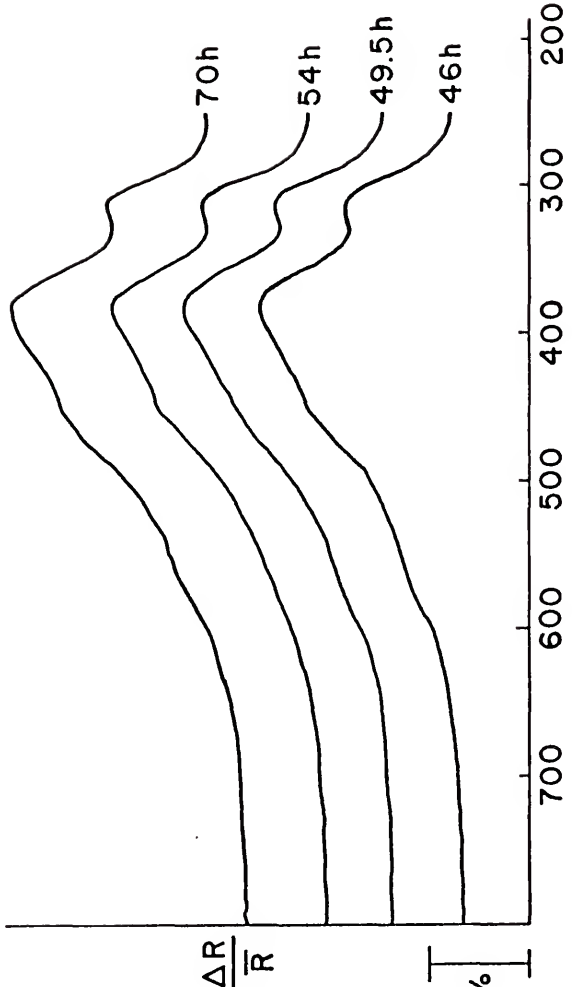

Figure 30. Continuation of the *in situ* experiment of Figure 29. Note the change in scale. Since the curves do not change appreciably during these times, the zero lines have been shifted for clarity.

which is generally not observed for Cu_2O in aqueous solutions.[20] Finally, few *in situ* experiments have shown a similar decrease in intensity. This implies that the initial anomalous intensity decrease is caused by the dissolution of a previously formed film, which may occasionally be produced under conditions such as lengthy exposure to the air, high humidity, and so on.

After about three hours, typical Cu_2O structure begins to appear. The amplitudes of the peak increase with time, and the curves more nearly approach those of "standard" Cu_2O patterns, which were not measured *in situ*.

The intensity of the mean peak near 385 nm as a function of time was fit to linear, power, logarithmic, and exponential functions by the method of least squares. The spectrum taken after three hours was used as a zero line because of the presumed dissolution of a previously formed film. The best fit was provided by a power curve of the form $\Delta R/\overline{R}[\%] = .62t^{.70}$ which had a correlation coefficient of $r^2 = .99$. If a theoretical curve of $\Delta R/\overline{R}$ versus thickness were available for Cu_2O as in the case of CuO (Figures 17 and 22) the kinetics of the growth of the oxide could be readily determined.

Experiments to monitor the growth of CuO films were not successful due to problems with breakdown of the

collodion protective layer after short exposure times. The relatively high potentials applied to the sample when it is potentiostated in the CuO region of the Pourbaix diagram appear to accelerate the onset of crevice corrosion under the film.

Further Discussion

When using the differential reflectometer in corrosion work, some way of matching the corrosion product and a specific differential reflectogram must be provided. Perhaps the most elegant method is to calculate the differential reflectogram from the optical constants and thickness of the film. This method, described in detail earlier in this section, works well when the optical constants of the film are known as a function of wavelength. If these data are not available, as in the case of Cu_2O, other methods must be employed to match the compounds and the spectra.

One technique is to potentiostat a sample well into a specific region of the Pourbaix diagram and assume that the predicted species is the one which is observed. This technique probably works well in most cases, but is rather limited from a research point of view.

Another is to grow a thick layer of some corrosion product, analyze it using X-ray diffraction techniques,

and correlate the results with a differential reflectogram of the film. Thinner films, which would have the same differential reflectogram, could be identified even though they themselves were too thin for X-ray analysis.

In order to test this idea, Cu_2O and CuO films were prepared by potentiostating copper in the normal manner for periods as long as a week. X-ray analyses at the University of Florida failed to detect any trace of the corrosion product. The samples were sent to Dr. B. Cavin at Oak Ridge National Laboratories where a special X-ray apparatus employing monochromatic X-rays and digital signal averaging techniques was used in an attempt to detect the films. After runs as long as seventy-two hours, the only X-ray lines which were observed other than those belonging to copper were the strongest line of Cu_2O and the strongest line of CuO. Both peaks were detected on both samples, and both peaks were so weak as to be barely distinguishable from background. It is likely that the time lag between the formation of the films and their measurement enabled both oxides to form on both samples. In any event, X-ray analysis does not seem to be a promising technique for confirming the identity of these films.

One final technique which may be used to confirm the identity of a corrosion product is to match its band

structure or optical reflection spectrum with structure evident in the differential reflectogram. This technique is useful in the case of Cu_2O, because of the extensive optical spectroscopy and band structure calculations which have been performed on that particular oxide.[20,30-32,35-47]

The band diagram of Cu_2O which is shown in Figure 5 reveals a band gap of 1.77 eV. According to these calculations the smallest energy for optical interband transitions should therefore be 1.77 eV. It is generally realized that the accuracy of band calculations is between 0.5 and 1 eV and depends strongly on the method of calculation and the input data. The experimental value for the band gap[20] was found to be 2.2 eV, which, in the light of the preceding statements, can be considered to be in fair agreement with the calculations.

The differential reflectogram of Cu_2O shown in Figure 13 shows structure at 2.25 eV which, as stated above, is identical to the energy associated with the band gap. Therefore, the structure at 2.25 eV can be tentatively attributed to the onset of interband transitions. From the calculated band diagram (Figure 5) one may deduce that the next set of interband transitions takes place approximately 1 eV above the threshold energy. This agrees with

our observations, where the second peak in the differential reflectogram occurs at 3.26 eV (380 nm).

Following this transition, the calculated band diagram (Figure 5) predicts a multitude of possible closely spaced transitions at higher energies. This is confirmed by the differential reflectogram (Figure 13) which shows complex and broad structure in the 3.4 to 5.4 eV energy interval (365 nm to 2300 nm).

Experimental reflectivity data, shown earlier in Table 2, shows essentially the same picture. Table 5 is a reproduction of Table 2 with the results of this study added for comparison. The results evident from this table, in addition to the prediction of the Pourbiax diagram and the results of the X-ray analysis, seem to establish beyond reasonable doubt that differential reflectograms typified by Figure 13 represent Cu_2O.

Another complicating factor which can cause errors in the analysis of thin film corrosion products when using optical techniques is the effect of surface roughening. The equations used in ellipsometry, or for that matter differential reflectometry, assume specular reflectance from the metal substrate. Surface roughening causes scattering of the light beam and can interfere with ellipsometric measurements. Presumably the same sort of

Table 5

Major Structure in Cu_2O Spectra Obtained from Other Techniques Compared to Differential Reflectometry

Reflectivity[36]	ε_2[36]	Electro-Reflectance Ref. 40	Electro-Reflectance Ref. 42	Calculated[32]	Differential Reflectometer (this study)
2.5	2.7	-	2.59 2.73	2.25 (1.77)	2.25
3.4	3.7	3.35 3.6	3.66 3.76	3.34 (2.86)	3.41
3.7	-	3.78 3.95	-	3.74 (3.26)	3.85
4.3	4.4	4.08 4.25	4.35 4.40	4.11 (3.63)	4.11
4.7	4.8	-	4.72 4.76 4.92	4.83 (4.35)	4.77
5.0	5.3	-	5.03 5.21	5.07 (4.59)	5.37

problems should exist with differential reflectometry. Surface roughening due to incomplete polishing causes no problem in differential reflectometry because both halves of the sample undergo the same polishing procedure, so any effect due to surface roughening should cancel out. However, roughening caused by electrochemical means acts only on the unprotected half of the specimen, and hence should contribute to the differential reflectogram. Since no peak shifts or additional structure were observed when samples were potentiostated for extended periods of time, however, it may be reasonably concluded that any surface roughening effects which did occur were insufficient to cause any significant changes in the differential reflectivity.

Recently a certain problem has arisen with regard to a few samples prepared potentiostatically when Miccroflex is used to protect the reference half of the sample. The differential reflectograms which are taken from these samples show Cu_2O structure, but with inverted polarity. This implies that the "protected" side of the sample is corroding preferentially and protecting the exposed side. The Cu_2O spectra are observed regardless of whether the sample is potentiostated in the Cu_2O or CuO area of the Pourbaix diagram. The reason appears to be a lack of adherence to

the copper by the Miccroflex, resulting in a concentration cell in the gap between the Miccroflex and copper. This increases the acidity of the electrolyte trapped under the Miccroflex and drives the covered area anodic with respect to the rest of the sample. Both effects tend to move the area covered with Miccroflex into the Cu_2O area of the Pourbaix diagram. This results in a film of Cu_2O being formed on the supposedly "clean" half of the sample, while the exposed half of the sample is relatively protected. The solution to the problem is simply to obtain fresh lacquer.

Finally, it was mentioned in Section II that electroreflectance effects can complicate thin film corrosion studies which employ modulation spectroscopy. Effects due to modulation of the electrode potential, such as are observed in electrochemical modulation spectroscopy (EMS), are of no concern here since the sample potential is not modulated. Effects due to the electric field emanating from a sample which has a DC charge on it have also been observed.[22,27] This field alters the optical constants of the electrolyte near the sample surface, and could affect measurements made *in situ*. However, the electric field surrounding the samples used in these experiments must be fairly uniform, particularly near the

center of the flat face which is being observed. Here again the differential nature of the technique would tend to cancel out any modifications to the index of refraction of the electrolyte, which must be small in any event. The fact that there is no additional structure in Figure 27B (measured *in situ*) compared to Figure 27A (not measured *in situ*) seems to confirm this reasoning.

SECTION V
CONCLUSIONS AND SUGGESTIONS FOR FURTHER WORK

It is hoped that this work shows that the application of differential reflectometry to the study of corrosion phemonema, even at its present early stage of development, can serve as a valuable supplement to the more established techniques of corrosion science. It has been shown that differential reflectometry can verify the existence and identity of thin film corrosion products on metal substrates. Different corrosion products have been shown to produce unique differential reflectograms, which can be qualitatively predicted from reflectivity data and band diagrams, or quantitatively predicted from the optical constants of the film. As in the case of ellipsometry, the thickness of the film may be determined if the optical constants are known. The technique is most useful in the film thickness range 0 to 200 Å, which covers the range of most passive and semipassive films. This range is often too thick for most surface analysis techniques which do not require a vacuum, and too thin for X-ray analysis.

Finally, it has been shown that differential reflectometry is capable of *in situ* measurements of thin film

corrosion products. More importantly, the electrolyte does not add additional structure to complicate the analysis, so measurements in optically dense electrolytes are possible.

There are many interesting possibilities for future research. For example, the well-established techniques of compositional modulation[48-51] can be used to investigate dealloying, especially the dezincification of brass. Small compositional changes, which are difficult to measure using conventional techniques, could be easily monitored in real time while the sample was still in the electrolyte. In order to facilitate such *in situ* studies, additional work needs to be performed on the development of transparent, protective coatings for the reference half of the sample. They must be able to be applied thinly and evenly, and must have uniformly low absorption throughout the range of the instrument as well as being immune to attack by the electrolyte.

More calibration curves of film thickness versus differential reflectivity need to be calculated. The curves for CuO shown in Figures 17 and 22 were calculated for a wavelength of 600 nm, but any wavelength within the range of the instrument could be used. In retrospect a wavelength of approximately 400 nm would be better for

the case of CuO, since the differential reflectivity is higher at that wavelength than at 600 nm for all thicknesses in the range of interest. As a consequence, greater precision could be obtained in the determination of the thickness of a film. Similarly, the calibration curve should be made near the strong peak at 385 nm in the case of Cu_2O, when the optical constants of that compound are determined. Wavelengths shorter than approximately 300 nm should be avoided, since the output of the Xenon light source is not strong in that area.

Additional metal/electrolyte systems could be investigated using differential reflectometry, with the aim of developing experimental Pourbaix diagrams for commercial alloys whose theoretical Pourbaix diagrams are not easily calculated. Here the technique can be a valuable supplement to electrochemical techniques, especially when the corrosion product cannot be exposed to vacuum.

REFERENCES

1. M. Fontana and N. Green, Corrosion Engineering (McGraw-Hill, New York, 1967) 28.

2. E. D. Verink, Jr., personal communication.

3. B. D. Cahan and R. F. Spanier, Surface Sci. 16 (1969) 166.

4. J. A. Holbrook and R. E. Hummel, Rev. of Sci. Instr. 44 (1973) 463.

5. E. D. Verink, Jr., and M. Pourbaix, Corrosion 27 (1971) 495.

6. P. C. Ladelfe, A. W. Czanderna, and J. R. Biegen, Thin Solid Films 10 (1972) 403.

7. O. S. Heavens, Optical Properties of Thin Solid Films (Dover, New York, 1965).

8. W. K. Paik and J. O'M. Bockris, Surface Sci. 28 (1971) 61.

9. R. C. O'Handley, Surface Sci. 46 (1974) 24.

10. R. C. O'Handley and D. K. Burge, Surface Sci. 48 (1975) 214.

11. S. Gottesfeld and B. Reichman, Surface Sci. 44 (1974) 377.

12. Gaertner Scientific Co., Chicago, Ill., Bulletin EH.

13. Gaertner Scientific Co., Chicago, Ill., Bulletin EA203-76P.

14. S. N. Jasperson, D. K. Burge, and R. C. O'Handley, Surface Sci. 37 (1973) 548.

15. H. J. Mathieu, D. E. McClure, and R. H. Muller, Rev. Sci. Instr. 45 (1974) 798.

16. R. M. A. Azzam, Rev. Sci. Instr. 47 (1976) 624.

17. J. D. E. McIntyre and D. M. Kolb, Symposium of the Faraday Society 4 (1970) 99.

18. J. D. E. McIntyre and D. E. Aspnes, Surface Sci. 24 (1971) 417.

19. D. M. Kolb and J. D. E. McIntyre, Surface Sci. 28 (1971) 321.

20. J. Kruger, J. Electrochem. Soc. 108 (1961) 503.

21. S. Matsuda, K. Sugimoto, and Y. Sawada, Trans. Japan Inst. Metals 18 (1977) 66.

22. J. D. E. McIntyre, Surface Sci. 37 (1973) 658.

23. J. D. E. McIntyre and W. F. Peck, Jr., in: Advances in Electrochemistry and Electrochemical Engineering, Vol. 9, Ed. R. H. Muller (Wiley-Interscience, New York, 1973) 66.

24. J. D. E. McIntyre, in: Optical Properties of Solids - New Developments, Ed. B. O. Seraphin (North Holland, New York, 1976) 555.

25. B. D. Cahan, J. Horkans, and E. Yeager, Surface Sci. 37 (1973) 559.

26. J. Horkans, B. D. Cahan, and E. Yeager, Surface Sci. 46 (1974) 1.

27. J. D. E. McIntyre and W. F. Peck, Jr., Faraday Disc. Chem. Soc. 56 (1973) 122.

28. W. R. Hansen, in: Progress in Nuclear Energy, Series IX, Anal. Chem., Vol. 11, Emittance and Reflectance Spectroscopy, Eds. H. A. Elion and D. C. Stewart (Pergamon, New York) 1.

29. J. D. E. McIntyre and W. F. Peck, Jr., in: Proc. Symp. on Electrocatalysts, San Francisco, 1974, Ed. M. W. Breiter (The Electrochemical Society, Princeton) 212.

30. A. G. Zhilich and V. P. Makarov, Soviet Phys. Solid St. 3 (1961) 429.

31. R. J. Elliott, Phys. Rev. 124 (1961) 340.

32. J. P. Dahl and A. C. Switendick, J. Phys. Chem. Solids 27 (1966) 931.

33. W. Kohn and N. Rostoker, Phys. Rev. 94 (1954) 1111.

34. J. C. Slater, Phys. Rev. 51 (1937) 846.

35. S. Brahms and S. Nikitine, Solid State Comm. 3 (1965) 209.

36. M. Balkasanski, Y. Petroff, and D. Trivich, Solid State Comm. 5 (1967) 85.

37. B. Prevot, C. Carabatos, and M. Seiskind, Phys. Stat. Sol. 10 (1972) 455.

38. M. Zouaghi, Phys. Stat. Sol. 11 (1972) 219.

39. M. Zouaghi, B. Prevot, C. Carabatos, and M. Seiskind, Phys. Stat. Sol. 11 (1972) 449.

40. S. N. Shestatskii and V. V. Sobolev, Phys. Stat. Sol. 32 (1969) K109.

41. S. N. Shestatskii, V. V. Sobolev, and N. P. Likhobabin, Phys. Stat. Sol. 42 (1970) 669.

42. A. Daunois, J. L. Deiss, and S. Nikitine, Solid State Comm. 10 (1972) 649.

43. Y. Ebisuzaki, J. Applied Phys. 32 (1961) 2027.

44. H. Wieder and A. W. Czanderna, J. Phys. Chem. 66 (1962) 816.

45. J. Kruger, J. Electrochem. Soc. 106 (1959) 847.

46. J. Kruger, J. Electrochem. Soc. 111 (1964) 1038.

47. D. J. G. Ives and A. E. Rawson, J. Electrochem. Soc. 109 (1962) 458.

48. R. E. Hummel, J. A. Holbrook, and J. B. Andrews, Surface Sci. 37 (1973) 717.

49. R. E. Hummel and J. B. Andrews, Phys. Rev. B 8 (1973) 2449.

50. R. J. Nastasi-Andrews and R. E. Hummel, Phys. Rev. B, in press.

51. R. Enderlein, R. E. Hummel, J. B. Andrews, R. J. Nastasi-Andrews, and C. W. Shanley, to be published.

52. M. Pourbaix, Atlas of Electrochemical Equilibria in Aqueous Solutions, First English Edition (Pergamon Press, Oxford, 1966).

53. Thaddeus S. Lee, Master's Thesis, University of Florida, 1972.

54. L. G. Schulz, J. Op. Soc. American, 44 (1954) 357.

55. L. G. Schulz and F. R. Tangherlini, J. Op. Soc. America 44 (1954) 362.

56. D. Halliday and R. Resnick, Physics (Wiley, New York, 1968) 1086.

57. M. Hansen, Constitution of the Binary Alloys (McGraw-Hill, New York, 1958).

BIOGRAPHICAL SKETCH

Charles William Shanley was born March 20, 1949, in Chicago, Illinois. He attended Loyola Academy in Wilmette, Illinois, where he graduated in 1967. Beginning in 1967, the author studied physics at the University of Dayton, Dayton, Ohio, where he graduated with a Bachelor of Science degree in 1971. He entered the graduate school at the University of Dayton in the field of materials science in 1971, and graduated in 1973 with a Master of Engineering degree. The author entered graduate school at the University of Florida in June, 1973, in the field of materials science and engineering. He received the degree of Master of Science in March, 1975, and has pursued the degree of Doctor of Philosophy since that date.

The author is a member of the American Institute of Mining, Metallurgical, and Petroleum Engineers, the American Society for Metals, and Alpha Sigma Mu.

I certify that I have read this study and that in my opinion it conforms to acceptable standards of scholarly presentation and is fully adequate, in scope and quality, as a dissertation for the degree of Doctor of Philosophy.

R. E. Hummel, Chairman
Professor of Materials
Science and Engineering

I certify that I have read this study and that in my opinion it conforms to acceptable standards of scholarly presentation and is fully adequate, in scope and quality, as a dissertation for the degree of Doctor of Philosophy.

J. J. Hren
Professor of Materials
Science and Engineering

I certify that I have read this study and that in my opinion it conforms to acceptable standards of scholarly presentation and is fully adequate, in scope and quality, as a dissertation for the degree of Doctor of Philosophy.

E. D. Verink, Jr.
Professor of Materials
Science and Engineering

I certify that I have read this study and that in my opinion it conforms to acceptable standards of scholarly presentation and is fully adequate, in scope and quality, as a dissertation for the degree of Doctor of Philosophy.

R. Pepinsky
Professor of Physics

This dissertation was submitted to the Graduate Faculty of the College of Engineering and to the Graduate Council, and was accepted as partial fulfillment of the requirements for the degree of Doctor of Philosophy.

December 1977

Dean, College of Engineering

Dean, Graduate School

UNIVERSITY OF FLORIDA
3 1262 08553 1126